

NACA RM L57E27

C.2



RESEARCH MEMORANDUM

EFFECTS OF CONTROL

PROFILE ON THE OSCILLATING HINGE-MOMENT AND FLUTTER

CHARACTERISTICS OF A FLAP-TYPE CONTROL

AT TRANSONIC SPEEDS

By William C. Moseley, Jr., and George W. Price, Jr.

Langley Aeronautical Laboratory
Langley Field, Va.

LIBRARY COPY

AUG 26 1957

LANGLEY AERONAUTICAL LABORATORY
LIBRARY, NACA
LANGLEY FIELD, VIRGINIA

CLASSIFIED DOCUMENT

This material contains information affecting the National Defense of the United States within the meaning of the espionage laws, Title 18, U.S.C., Secs. 793 and 794, the transmission or revelation of which in any manner to an unauthorized person is prohibited by law.

NATIONAL ADVISORY COMMITTEE FOR AERONAUTICS

WASHINGTON

August 23, 1957



3 1176 01438 1033

NATIONAL ADVISORY COMMITTEE FOR AERONAUTICS

RESEARCH MEMORANDUM

EFFECTS OF CONTROL

PROFILE ON THE OSCILLATING HINGE-MOMENT AND FLUTTER

CHARACTERISTICS OF A FLAP-TYPE CONTROL

AT TRANSONIC SPEEDS

By William C. Moseley, Jr., and George W. Price, Jr.

SUMMARY

Free-oscillation tests were made in the Langley high-speed 7- by 10-foot tunnel to determine the effects of control profile on the dynamic hinge-moment and flutter characteristics of a trailing-edge flap-type control. A conventional control and two control profile modifications were tested. The essentially full-span controls were 22.2 percent of the wing chord and had overhang nose balances equal to 35 percent of that portion of the control chord rearward of the hinge line. Test parameters included a Mach number range from 0.60 to 1.01, control oscillation amplitudes up to about 13° , and a range of control reduced frequencies. Static hinge-moment data were also obtained for the three control profiles tested.

Results indicate that the unstable aerodynamic damping for the conventional control at Mach numbers from 0.90 to 1.01 (maximum for these tests) was not beneficially affected by the "splitter-plate" modification tested. In general, the "splitter-plate" control gave dynamic hinge-moment results very similar to those for the conventional control throughout the complete test range. The wedge-control modification did beneficially affect the aerodynamic damping moments and resulted in stable damping at low oscillation amplitudes for the entire Mach number range. However, this beneficial effect was confined to oscillation amplitudes of less than about 3° ; for oscillation amplitudes greater than about 3° the aerodynamic damping was unstable in the Mach number range from 0.92 to 1.01. A self-excited flutter involving only rotation of the control about the hinge line was associated with the unstable damping for all three controls. Flutter for the conventional and "splitter-plate" controls was initiated by random tunnel disturbances, while for the wedge control, a manual displacement to an oscillation amplitude of about 4° was necessary before flutter would occur. Thickening the control trailing edge caused the control to become more underbalanced at Mach numbers below 0.90, and for all three controls the static and dynamic spring-moment derivatives varied with Mach number in much the same manner.

INTRODUCTION

There is a need for dynamic hinge-moment information on flap-type controls at transonic speeds. The data are important in flutter studies and in the design of control servo systems. Previous investigations have generally shown the aerodynamic damping in the control rotational mode to be unstable at transonic speeds (see, for example, ref. 1), and a single-degree-of-freedom flutter of the control can exist if this unstable aerodynamic damping exceeds the stable damping from other sources in the control system. This instability is sometimes called control-surface buzz and usually means that some form of artificial damping must be added to the control system for dynamic stability. Adding this damping generally leads to mechanical complexities, and it would be desirable to stabilize the control aerodynamically by some relatively simple geometric change, provided overall control efficiency can be maintained.

The investigations reported in references 2 and 3 were made on a low-aspect-ratio unswept-wing-control model to study the effects of control hinge-line position and one trailing-edge thickness modification on the dynamic hinge moments at transonic speeds. The investigation of reference 4 was made on a low-aspect-ratio delta-wing-control model with a conventional control and a thickened trailing-edge control. No significant benefits in aerodynamic damping were obtained for the parameters varied in these reference tests. The present investigation was made on the model used in references 2 and 3 for one control hinge position previously reported in the hope that favorable damping could be realized from some additional profile modification. The flap-type controls reported herein include a conventional profile, a wedge profile wherein the trailing edge is thicker than the control leading edge, and a so-called "splitter-plate" control. This latter profile arrangement evolved from a flight investigation to improve control dynamic characteristics (ref. 5) and essentially replaces the rear portion of the control chord with a thin plate.

In the present investigation a free-oscillation test technique was used and oscillating hinge moments together with associated flutter characteristics were determined at an angle of attack of 0° for the following conditions: a range of control reduced frequencies, initial oscillation amplitudes up to 13° , and a Mach number range from 0.60 to 1.01. In addition, static hinge moments were obtained for all three controls.

SYMBOLS

C_h	control hinge-moment coefficient, $\frac{\text{Hinge moment}}{2M'q}$
$M_{\delta, \omega}$	aerodynamic hinge moment on control per unit deflection, positive trailing edge down, ft-lb/radian
q	free-stream dynamic pressure, lb/sq ft
M'	area moment of aileron area rearward of and about hinge line, cu ft
c	local wing chord, ft
c_a	control chord (distance from hinge line rearward to trailing edge of control, see fig. 2), ft
c_b	balance chord (distance from hinge line forward to leading edge of control (see fig. 2)), ft
c_t	total control chord, $c_b + c_a$, ft
k	reduced frequency, $\frac{\omega c_t}{2V}$, c_t taken at midspan of control
ω	angular frequency of oscillation, $2\pi f$, radians/sec
V	free-stream velocity, ft/sec
f	frequency of oscillation, cycles/sec
f_0	control wind-off natural frequency, cycles/sec
I	moment of inertia of control system, slug-ft ²
λ	logarithmic decrement, $\frac{d(\log \delta_1)}{d(\text{Time})}$, per sec
δ_1	amplitude of oscillation, deg to each side of mean
δ	control-surface deflection, measured in a plane perpendicular to control-surface hinge line, positive when control-surface trailing edge is below wing chord plane, radians except as noted

- M effective Mach number over span of model, $\frac{2}{S_1} \int_0^{b/2} cM_a dy$
- S_1 twice wing area of semispan model, sq ft
- b twice span of semispan model, ft
- M_a average chordwise local Mach number
- M_z local Mach number
- y spanwise distance from plane of symmetry, ft

$$C_{h\delta} = \frac{\partial C_h}{\partial \delta}$$

$$C_{h\dot{\delta}} = \frac{\partial C_h}{\partial \left(\frac{\dot{\delta} c_t}{2V} \right)}$$

$$C_{h\delta, \omega} = \frac{\text{Real part of } M_{\delta, \omega}}{2M'q}, \text{ per radian}$$

$$C_{h\dot{\delta}, \omega} = \frac{\text{Imaginary part of } M_{\delta, \omega}}{2M'qk}, \text{ per radian}$$

- B "bumped" flutter condition; that is, flutter starts when control surface is manually displaced and suddenly released
- S "self-starting" flutter condition; that is, flutter starts when control surface is released without being manually displaced

Subscript:

- ω function of angular frequency of oscillation

MODEL AND APPARATUS

The model consisted of a wing, a trailing-edge flap-type control, and a control-system spring-deflector mechanism. A schematic drawing

of the test installation is shown in figure 1, and general dimensions of the model and controls tested are given in figure 2. Photographs of the test installation are presented as figure 3. The control system was designed so that its moment of inertia could be varied in order to measure the dynamic hinge moments and flutter characteristics for a range of control reduced frequency.

Wing Details

The wing had a full-span aspect ratio of 1.80, a taper ratio of 0.74, 0° sweep of the 0.40 chord line, and an NACA 64A004 airfoil section with a modified trailing edge. The portion of the wing rearward of the 0.70 chord line was modified so that the trailing edge had a thickness equal to 0.0036c. This modification was included for the present tests to be consistent with references 2 and 3.

The wing was constructed with a solid steel core and a plastic surface. All tests were made with a tip store attached to the wing, and stores of different weight were used to change the wing natural frequencies. The natural first bending and torsion frequencies of the wing with the two tip stores used are given in table I. These wing frequencies were obtained with the control system clamped (see fig. 4).

Control-System Details

The flap-type controls had a total chord c_t equal to 30 percent of the wing chord and extended from the $0.086b/2$ wing station to the $0.943b/2$ wing station. The control had a $0.35c_a$ blunt overhang nose balance, and the gap between the control and wing was unsealed. Three control profiles were tested (fig. 2(b)). One profile conformed to the airfoil section tested and is referred to hereinafter as the conventional control. The second control had a "splitter-plate" type of modification wherein the rearward 50 percent of the control chord c_a was equal to the trailing-edge thickness except for five equally spaced chordwise stiffeners. The third control had a thickened trailing edge wherein the trailing-edge thickness was $1\frac{1}{2}$ times the hinge-line thickness. This control, which is referred to as the "wedge control," had straight sides from the nose radius to the trailing edge. Consequently, the hinge-line thickness is slightly greater than for the conventional control. The plain control and the splitter-plate control were made of solid steel, and the wedge control had a steel spar with spruce afterportion. In order to mass-balance the controls about the hinge line, tungsten inserts were distributed in the overhang to balance as nearly as possible each spanwise segment of the control. For the solid-steel controls it was

necessary to drill holes rearward of the hinge line to mass balance the controls completely. These holes were plugged with balsa and the control surface covered with silk.

The inboard tang of the control extended through the reflection plane to the outside of the tunnel (fig. 3). The tang extension consisted of a rod and a torsion spring. The control was mounted by two ball bearings outside the tunnel and a plain bearing at the wing tip. System alignment was carefully checked to keep friction to a minimum. Attached to the rod were a small armature which rotated in the magnetic field of a reluctance-type pickup to indicate control position and a deflector arm used to apply a step deflection to the control system. The natural frequency of the control system was varied by changing the moment of inertia of the control system, by clamping two weights of different size and inertia to the rod. Values of natural frequency given in figure 4 are for the three control-system inertias for each control profile tested. The moments of inertia of the control system for the three control profiles tested are given in table II.

Instrumentation

Strain gages were located near the root of the wing to indicate the wing bending and torsion responses. Control position was measured by a reluctance-type pickup located on the tang extension near the inboard end of the control. Outputs of these three quantities were recorded against time by a recording oscillograph. Dynamic calibration of the recording system indicated accurate response to a frequency of about 500 cycles per second.

TESTS

The tests were made in the Langley high-speed 7- by 10-foot tunnel utilizing the sidewall reflection-plane test technique. This technique involves mounting a relatively small model on a reflection plate spaced out from the tunnel wall to bypass the tunnel boundary layer. Local velocities over the surface of the test reflection plate allowed testing to a Mach number of 1.01 without choking the tunnel.

Typical contours of local Mach number in the vicinity of the model location, obtained with no model in place, are shown in figure 5. Average test Mach numbers were obtained from similar contour charts by using the relationship

$$M = \frac{2}{S_1} \int_0^{b/2} cM_a dy$$

The tunnel stagnation pressure was essentially equal to sea-level atmospheric conditions.

The variation of Reynolds number based on the wing mean aerodynamic chord with test Mach number is presented in figure 6. The width of the band in figure 6 represents the maximum variation of Reynolds number with atmospheric conditions for these tests at a given Mach number.

Oscillating hinge moments were obtained for the three control profiles throughout a Mach number range of 0.60 to 1.01 for initial amplitudes up to about 13° . The control reduced frequency range varied with Mach number and control-system inertia and was generally in the range from 0.05 to 0.20. In addition, static hinge moments were obtained for the three control profiles. All tests were made at a wing angle of attack of 0° .

TEST TECHNIQUE AND REDUCTION OF DATA

Oscillating hinge moments were obtained from the free-oscillation response of the control system. The control system was designed so that at the test frequencies the torsional response of the control about the hinge line was essentially that of a single-degree-of-freedom system. The wing response characteristics were varied relative to the control oscillating frequency by the tip stores so that the physical response of the model for the various test conditions was predominantly control rotation. Therefore, the aerodynamic moment resulting from angular deflection of the control about the hinge line could be determined from the free-oscillation characteristics of the control system following known starting conditions. Typical oscillograph records of the time response of the model are shown in figure 7.

The technique used to initiate the free oscillations depended on the total damping (aerodynamic plus nonaerodynamic) of the control system for the particular test condition. When the total damping was unstable at low deflections, the hinge moments were determined from the unstable oscillation following release of the control at $\delta = 0$ (fig. 7(c)). This type of oscillation was initiated by random tunnel disturbances and in all cases was self-limiting because of the nonlinear variation of aerodynamic damping with oscillating amplitude. When the total damping was stable or varied from stable to unstable within the test oscillation-amplitude range, the free oscillation was initiated by releasing the control at zero initial rotational velocity at some deflection angle (figs. 7(a) and (b)). The ensuing oscillation was either a buildup or a decay, and, for the conditions where the damping varied from stable to unstable, the initial deflection or release angle was varied so as to study the complete oscillation-amplitude range.

The hinge moment existing on an oscillating control is not necessarily in phase with the control position and may be represented in complex notation by the relation

$$\frac{M_{\delta,\omega}}{2M'q} = C_{h_{\delta,\omega}} + ikC_{h_{\delta,\omega}} \quad (1)$$

The part $C_{h_{\delta,\omega}}$ is proportional to the real component of the moment which is commonly called the in-phase or spring moment. The part $kC_{h_{\delta,\omega}}$ is proportional to the imaginary component of the moment which is commonly called the out-of-phase or damping moment. Frequency effects higher than the first order could not be separated by the test method used in this investigation; therefore, the parameters $C_{h_{\delta,\omega}}$ and $kC_{h_{\delta,\omega}}$ include the higher order derivatives that are either in phase or out of phase, respectively, with control position.

Evaluation of Spring Moments

The aerodynamic in-phase or spring moment was determined from the natural frequency of oscillation of the control system. Since the variation of in-phase moment is not necessarily linear with amplitude and the test method was not sufficiently accurate to determine the variation in natural frequency with amplitude, the values of $C_{h_{\delta,\omega}}$ presented are effective values averaged over the amplitude range of the oscillation. The effect of the values of damping encountered in this investigation on the natural frequency were considered negligible and the aerodynamic spring-moment derivative was determined from the relationship

$$C_{h_{\delta,\omega}} = \frac{I(\omega_0^2 - \omega_1^2)}{2M'q} \quad (2)$$

where the subscript 0 signifies a wind-off condition. As shown by equation (2), negative values of $C_{h_{\delta,\omega}}$ oppose the control displacement and hence increase the stiffness or natural frequency of the control system.

Evaluation of Damping Moments

The aerodynamic out-of-phase or damping moment was determined from the rate of buildup or decay of the free oscillation of the control system. The damping moment is not necessarily linear with amplitude;

however, the damping results were analyzed on the basis of an equivalent linear system. It was assumed that the damping forces were adequately described by an equivalent viscous damping and that the time response of the actual system was simulated by a linear system having the appropriate damping constant at each oscillating amplitude for a given frequency. The variation of damping-moment derivative with oscillating amplitude was obtained by plotting the logarithm of the amplitude of successive cycles of the oscillation against time and taking the slope at any given amplitude of the faired curve as the value of the logarithmic decrement $\lambda = \frac{d(\log \delta_1)}{d(\text{Time})}$ of the oscillation. The aerodynamic damping derivative was determined from the relationship

$$C_{h;\delta,\omega} = \frac{2IV}{qM'c_t} (\lambda - \lambda_0) \quad (3)$$

where the subscript 0 refers to wind-off values taken at approximately the same frequency and amplitude as the wind-on values.

Determination of Static Hinge Moments

Static hinge moments were measured by attaching to the control-system rod extension a bracket which was fitted with a calibrated electric strain gage which measured the torque or moment about the control hinge line for various control deflections. The static hinge-moment coefficient C_h was determined from the relationship

$$C_h = \frac{\text{Hinge moment}}{2M'q} \quad (4)$$

General Comments on Data

Values given for oscillating and flutter amplitudes are to each side of mean, and for this investigation the mean oscillating amplitude was very near zero deflection. Flutter in all cases was a limited-amplitude oscillatory condition and was terminated by physically restraining the control motion. For the free-oscillation technique used, the reduced frequency k varies with Mach number; values of k are given for each Mach number.

The wing bending and torsion traces shown in figure 7 are indications of the wing-root bending and torsion stresses, while the control-position trace indicates the control deflection. The traces in figures 7(a) and 7(b) were more sensitive than those in figure 7(c). Elimination of all wing motion in an investigation of this type is desirable

but not practical; however, care was taken to minimize the wing motion. The control surface was dynamically balanced about the hinge line to prevent inertia coupling between the wing and control due to control rotation. The wing was fitted with two tip stores of different mass to change the wing natural frequencies and hence control the wing response motion to the control induced aerodynamic forcing function. Wing bending and torsion responses of the general magnitude encountered in these tests were approximated by simple wing translation and rotation and analyzed by the theoretical methods presented in references 6 and 7. The effects of this wing motion on the calculated control hinge-moment parameters for a control hinged at the leading edge were very small. Therefore, in this investigation wing motion was considered to have only secondary effects on the control hinge-moment parameters.

CORRECTIONS

No corrections have been applied to the data for the chordwise and spanwise velocity gradients or for the effects of the tunnel walls. It is shown in reference 8 that a tunnel resonance phenomenon can appreciably decrease the magnitude of forces and moments measured in oscillation tests. However, it is believed that this phenomenon had no appreciable effect on the results of the present investigation. In general, most of the test frequencies were well removed from the calculated resonant frequencies, and there was no apparent decrease in moments for the test frequencies that were close to resonant frequencies. It is possible that the magnitude of the resonant effects would be relieved by the model tip effects and the nonuniformity of the velocity field in the test section.

Static-control-deflection corrections have been applied to the output of the position pickup to give the deflection at the midspan of the control surface. No dynamic corrections were applied to account for the twist of the control system outboard of the position pickup (fig. 4) since, for the physical constants and frequencies involved, this was a secondary effect and generally negligible.

RESULTS AND DISCUSSION

Damping Moments and Flutter Characteristics

The variation of aerodynamic damping coefficient $C_{h_{\delta, \omega}}$ with oscillating amplitude and Mach number together with the associated flutter characteristics are presented in figures 8 to 10 for the three control

profiles investigated. Parts (a), (b), and (c) of these figures represent data for the different control reduced frequencies investigated. Shown in figure 11 is a comparison of the damping results for the conventional control and wedge control.

Conventional control.- The aerodynamic damping results for the conventional control (fig. 8) indicate that the damping was stable for all amplitudes and reduced frequencies investigated at Mach numbers from 0.60 to about 0.90 and was unstable in the Mach number range from about 0.92 to 1.01, the maximum Mach number tested. In general, $C_{h\delta,\omega}$ was fairly constant to maximum test amplitudes of about 10^0 at the lower test Mach numbers ($M = 0.60$ to $M = 0.80$) and became less stable with increasing amplitude at the intermediate Mach numbers ($M = 0.85$ through $M = 0.90$). At the higher test Mach numbers ($M = 0.92$ through $M = 1.01$) maximum unstable values of $C_{h\delta,\omega}$ generally occurred at the lower oscillating amplitudes with unstable values of $C_{h\delta,\omega}$ decreasing with increase in amplitude, thus leading to the limited-amplitude type of flutter response obtained. For the conventional control changes in test oscillation amplitude did not change the general variation in $C_{h\delta,\omega}$ with Mach number.

When comparing the flutter characteristics with the aerodynamic damping values (fig. 8), it should be remembered that the control system had a certain level of nonaerodynamic damping. Flutter was a self-excited oscillation involving only the degree of freedom of control rotation about the hinge line. In all cases tested for this control, flutter was self-starting and built up in amplitude until a steady-state condition was reached, wherein the aerodynamic energy fed into the oscillation over a complete cycle was equal to the energy dissipated by nonaerodynamic damping (see fig. 7(c)). The flutter frequencies and amplitudes given are for the constant-amplitude oscillatory conditions for this model.

In the Mach number region where the aerodynamic damping was stable, variation within the reduced-frequency range investigated generally had small effects on the magnitude of $C_{h\delta,\omega}$ (see fig. 8). For the region where the aerodynamic damping was unstable the damping coefficient $C_{h\delta,\omega}$ tended to become slightly more unstable over the amplitude range as the test reduced frequency was decreased. In addition, the flutter amplitude increased with decrease in reduced frequency.

This conventional control was basically the same as the control having $c_b/c_t = 0.35$ reported in reference 3. In the reference investigation, the reduced frequency was generally varied by changing the

control torsional spring; in the present investigation, however, the length of the torsional spring was held constant and the control-system inertia changed. In both investigations, aerodynamic data were measured in essentially the same test range, and there is good agreement between the separate tests. This agreement indicates that the test techniques used can satisfactorily repeat the aerodynamic effects measured.

Splitter-plate control.- Aerodynamic damping results for the splitter-plate control (fig. 9) show that no beneficial effects were obtained with this control modification. Variations of $C_{h\delta,\omega}$ with Mach number and amplitude were generally similar to the conventional control; that is, the damping was generally stable at low Mach numbers ($M = 0.60$ to about $M = 0.90$) and generally unstable from $M = 0.92$ to $M = 1.01$, the maximum Mach number tested. Flutter was self-starting and built up until a constant-amplitude condition was reached, and flutter amplitudes were generally similar to those obtained for the conventional control. Differences in wind-off and wind-on frequencies for the conventional control and splitter-plate control were caused by differences in control system moment of inertia. (See table II.)

The flight investigation of reference 5 gave qualitative indication of improved "buzz stability" with a particular splitter-plate configuration. Direct comparison of the model and flight results is not feasible, however, since the aerodynamic damping was not measured in the flight tests. In addition, differences in sweep, thickness, and profile existed between the control of the present investigation and that flight-tested in reference 5.

Wedge control.- The wedge profile modification to the control did give some beneficial effects in aerodynamic damping at the transonic-speeds at which tests were made. Complete test results for this control are given in figure 10 and a representative comparison with the conventional control is made in figure 11. Damping for the wedge control (fig. 10) was stable at low oscillating amplitudes up to the maximum Mach number tested, although the variation of $C_{h\delta,\omega}$ with M was erratic at transonic test speeds. The region of stable damping was confined to oscillating amplitudes of less than about 3° ; however, this angle together with the level of unstable damping at the higher oscillation amplitudes depended on the oscillation reduced frequency and free-stream Mach number. Flutter in all cases for this wedge control was a "bumped" condition and the displacement amplitudes necessary to initiate the flutter can be approximated from figure 10. The nonaerodynamic damping of the control system was sufficient to prevent flutter at transonic speeds for the highest reduced frequencies tested (fig. 10(a)). The data of figure 11 illustrate the stable shift in damping due to the wedge modification at low oscillating amplitudes throughout the Mach number range tested. However, the damping and flutter results at high oscillating amplitude were not appreciably affected by the wedge modification to the control.

Spring Moments

Static hinge-moment or spring-moment coefficients are shown in figure 12 for the three control profiles tested. The variation of the static and dynamic spring-moment derivatives $C_{h\delta}$ and $C_{h\delta,\omega}$ with Mach number are shown in figure 13.

The variation of C_h with control deflection was very similar for the conventional and splitter-plate controls (figs. 12(a) and (b)) at all Mach numbers investigated. For these controls the variation of C_h with δ was generally linear and slightly underbalanced at low deflections and became more underbalanced at the higher deflections. In the Mach number range from 0.95 to 1.01 the variation of C_h with δ was generally linear over the entire deflection range, and the aerodynamic loading center shifted rearward so that the control was considerably underbalanced.

For the wedge control (fig. 12(c)) C_h varied with control deflection and Mach number in a manner similar to the conventional and splitter-plate controls; however, increasing the trailing-edge thickness results in an increase in the underbalance of the control at the lower test Mach numbers (from $M = 0.60$ to $M = 0.90$). Above $M = 0.90$ the increase in trailing-edge thickness had little effect and the variation of C_h with δ was similar for all three controls.

The spring-moment derivatives measured from static ($C_{h\delta}$) and dynamic ($C_{h\delta,\omega}$) tests are in qualitative agreement, for the three controls (fig. 13). Direct comparison of the static and dynamic results to determine the effects of oscillating frequency is not feasible since the derivatives could not be evaluated for the same amplitude range. For the test technique used, the dynamic derivatives in some cases were evaluated for an amplitude range where the static hinge-moment data become nonlinear with amplitude. However, results shown in figure 13 indicate that, for these controls, static data could be used to make fairly accurate frequency estimates for single-degree-of-freedom transonic control-surface flutter.

CONCLUSIONS

Results of tests made at Mach numbers from 0.60 to 1.01 to determine the effects of control profile on the oscillating hinge-moment and flutter characteristics of a flap-type control indicate the following conclusions:

1. The unstable aerodynamic damping for the conventional control at Mach numbers from 0.92 to 1.01 (maximum for these tests) was not beneficially affected by the "splitter-plate" modification tested. In general, the dynamic hinge-moment results for the "splitter-plate" control were similar to the results for the conventional control for the complete test range.

2. The wedge-control modification did beneficially affect the aerodynamic damping moments and resulted in stable damping at low oscillating amplitudes for the entire Mach number range. However, this beneficial effect was confined to oscillation amplitudes less than about 3° , and the damping was unstable for oscillation amplitudes greater than about 3° in the Mach number range from about 0.92 to 1.01.

3. A self-excited flutter involving only rotation of the control about the hinge line was associated with the unstable damping for all three controls. Flutter for the conventional and "splitter-plate" controls was initiated by random tunnel disturbances, while the wedge control had to be manually displaced to some amplitude greater than about 4° before flutter occurred.

4. Thickening the control trailing edge caused the control to become more underbalanced at Mach numbers below 0.90. For all three controls the static and dynamic spring-moment derivatives varied with Mach number in much the same manner.

Langley Aeronautical Laboratory,
National Advisory Committee for Aeronautics,
Langley Field, Va., May 3, 1957.

REFERENCES

1. Martin, Dennis J., Thompson, Robert F., and Martz, C. William: Exploratory Investigation of the Moments on Oscillating Control Surfaces at Transonic Speeds. NACA RM L55E31b, 1955.
2. Thompson, Robert F., and Moseley, William C., Jr.: Oscillating Hinge Moments and Flutter Characteristics of a Flap-Type Control Surface on a 4-Percent-Thick Unswept Wing With Low Aspect Ratio at Transonic Speeds. NACA RM L55K17, 1956.
3. Thompson, Robert F., and Moseley, William C., Jr.: Effect of Hinge-Line Position on the Oscillating Hinge Moments and Flutter Characteristics of a Flap-Type Control at Transonic Speeds. NACA RM L57C11, 1957.
4. Martz, C. William: Experimental Hinge Moments on Freely Oscillating Flap-Type Control Surfaces. NACA RM L56G20, 1956.
5. Anon.: Flight Test Progress Report No. 23 for Period Ending 7 October 1955 for Model FJ-4 Airplanes. Report No. NA 54H-374-23 (Contract NOa(s) 54-323), North American Aviation, Inc., Oct. 20, 1955.
6. Anon.: Tables of Aerodynamic Coefficients for an Oscillating Wing-Flap System in a Subsonic Compressible Flow. Rep. F.151, Nationaal Luchtvaartlaboratorium, Amsterdam, May 1954.
7. Nelson, Herbert C., and Berman, Julian H.: Calculations on the Forces and Moments for an Oscillating Wing-Aileron Combination in Two-Dimensional Potential Flow at Sonic Speed. NACA Rep. 1128, 1953. (Supersedes NACA TN 2590.)
8. Runyan, Harry L., and Watkins, Charles E.: Considerations on the Effect of Wind-Tunnel Walls on Oscillating Air Forces for Two-Dimensional Subsonic Compressible Flow. NACA Rep. 1150, 1953. (Supersedes NACA TN 2552.)

TABLE I

NATURAL FIRST BENDING AND TORSION FREQUENCIES OF WING

Test condition	Bending, cps	Torsion, cps
Light tip store	141	490
Heavy tip store	85.5	232

TABLE II

MOMENTS OF INERTIA OF CONTROL SYSTEMS

Control system	I, slug-ft ²
Plain control	1.45×10^{-5}
Plain control plus small inertia weight	3.40
Plain control plus large inertia weight	11.25
"Splitter-plate" control	1.71
"Splitter-plate" control plus small inertia weight	3.66
"Splitter-plate" control plus large inertia weight	11.51
Wedge control	1.56
Wedge control plus small inertia weight	3.51
Wedge control plus large inertia weight	11.36

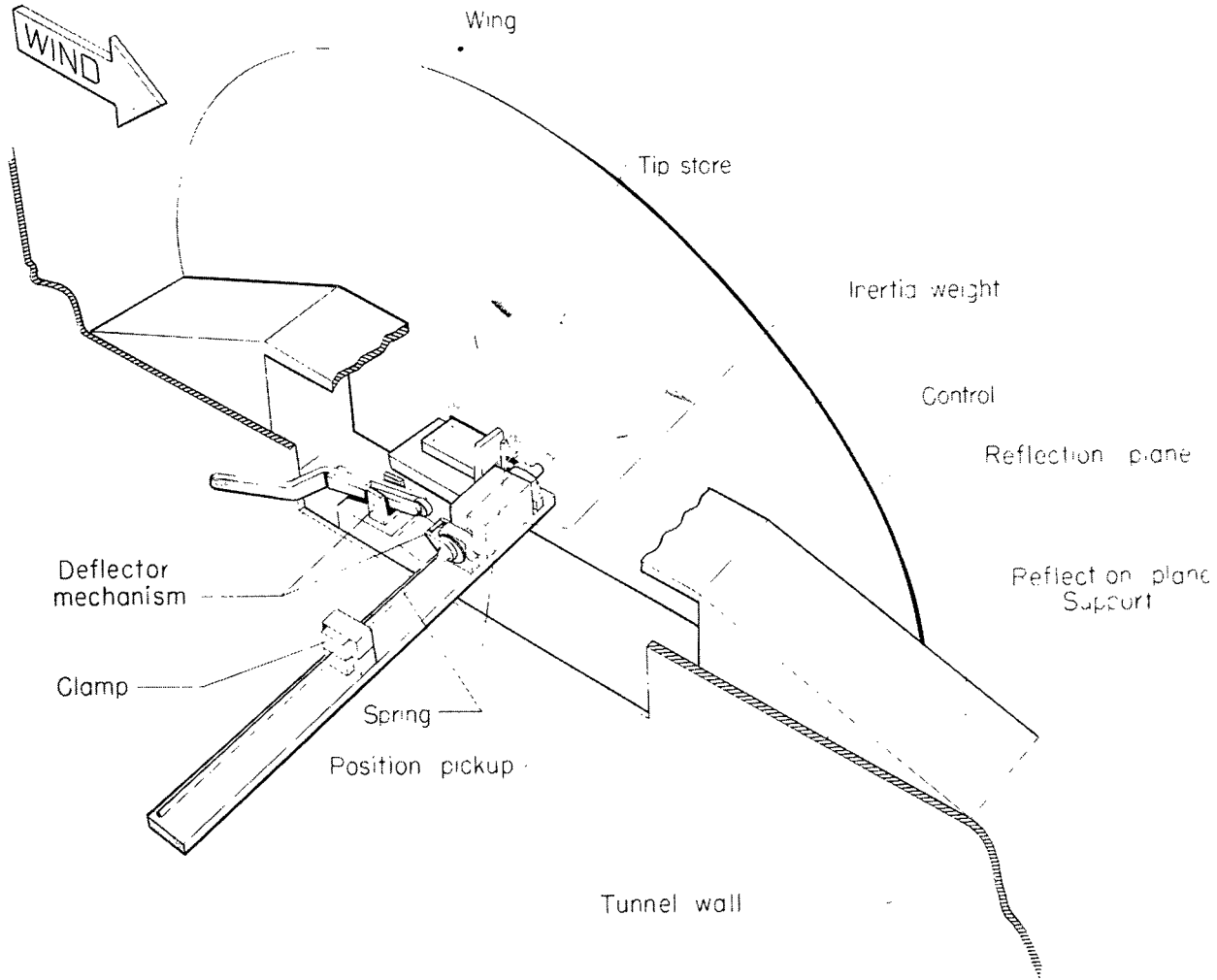
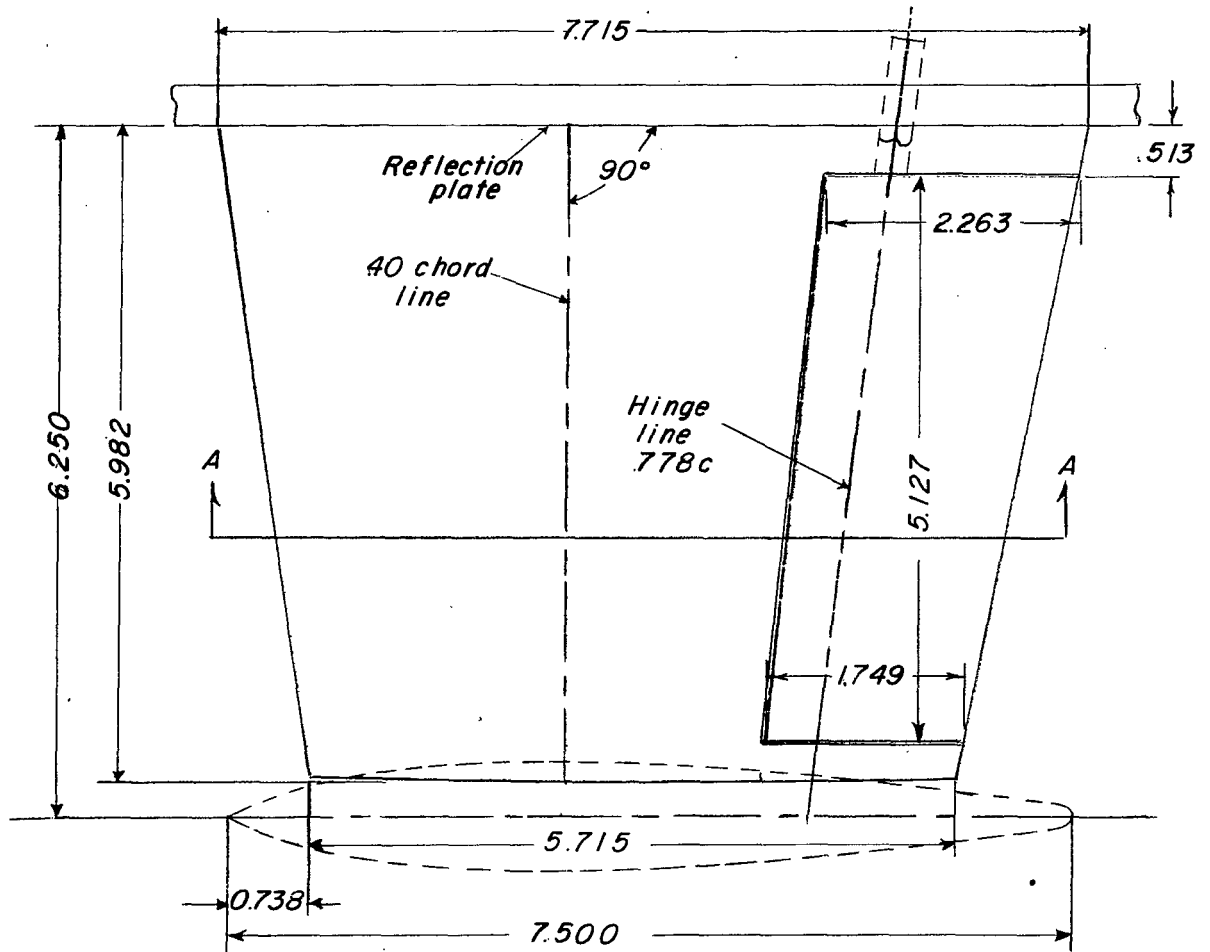


Figure 1.- Schematic drawing of test installation. L-90563.2



Tabulated Wing Data

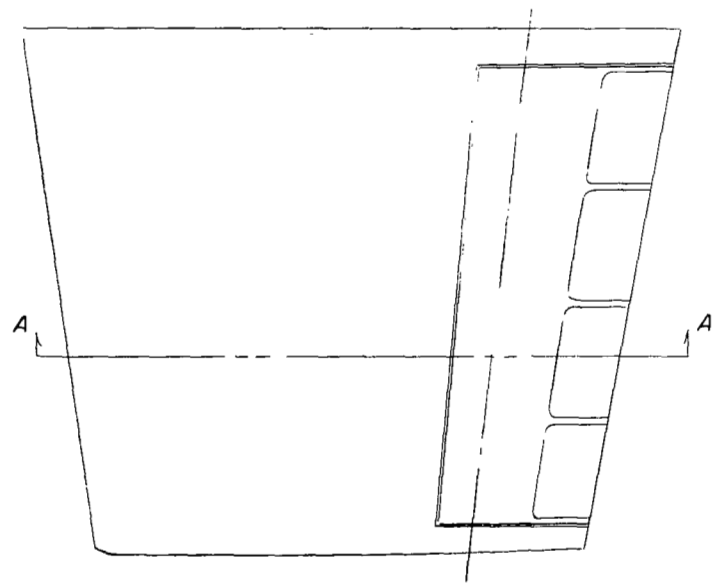
Area	0.558 sq ft
Aspect ratio	1.80
Taper ratio	0.74
Mean aerodynamic chord	0.564 ft
Airfoil section parallel to free stream	NACA 64A004 (modified)



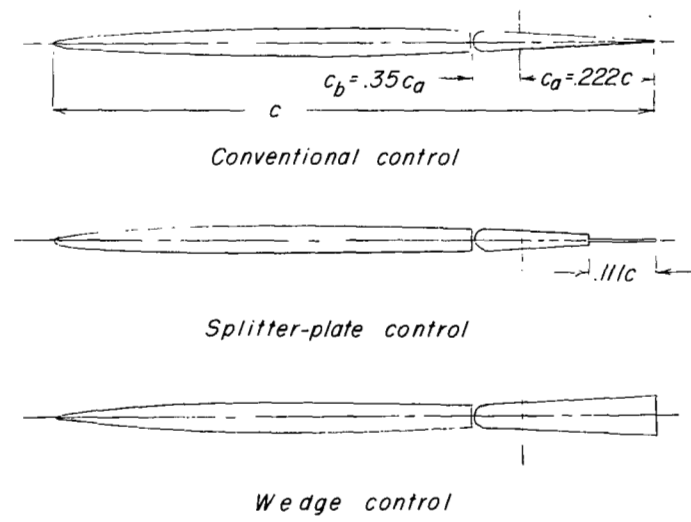
Scale, inches

(a) Plan form of model. Conventional control.

Figure 2.- General dimensions of test model.



Plan form showing splitter-plate control



Conventional control

Splitter-plate control

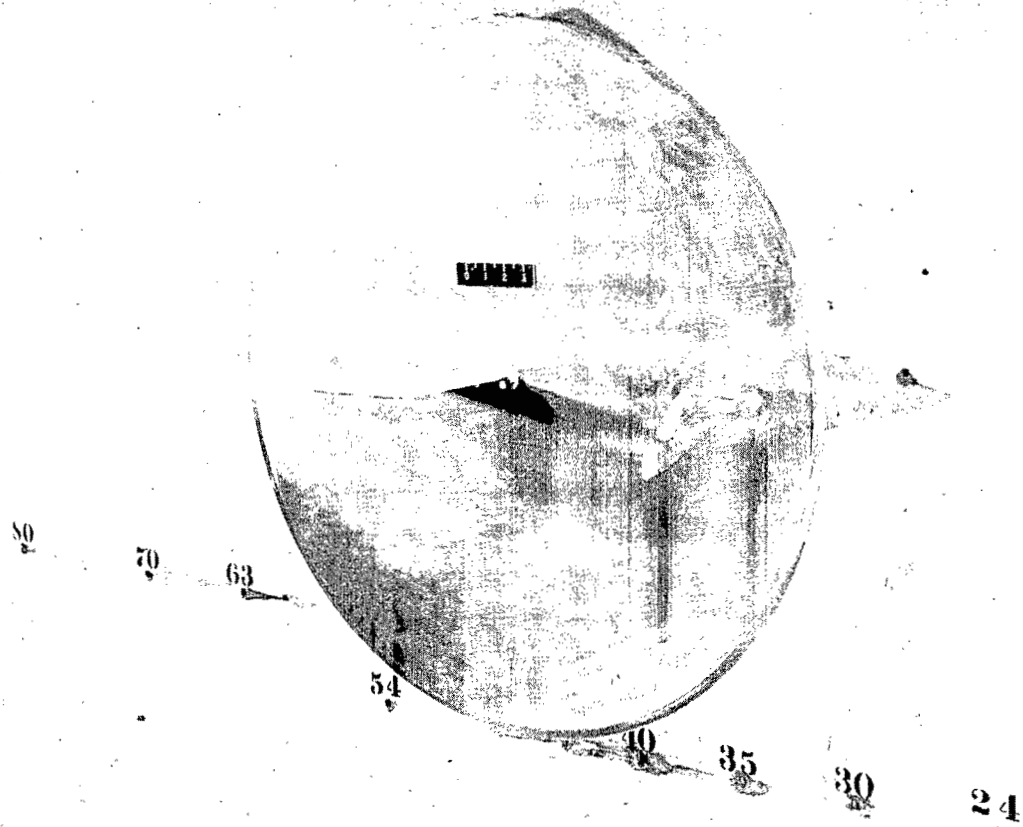
Wedge control

Section AA

For three control profiles tested

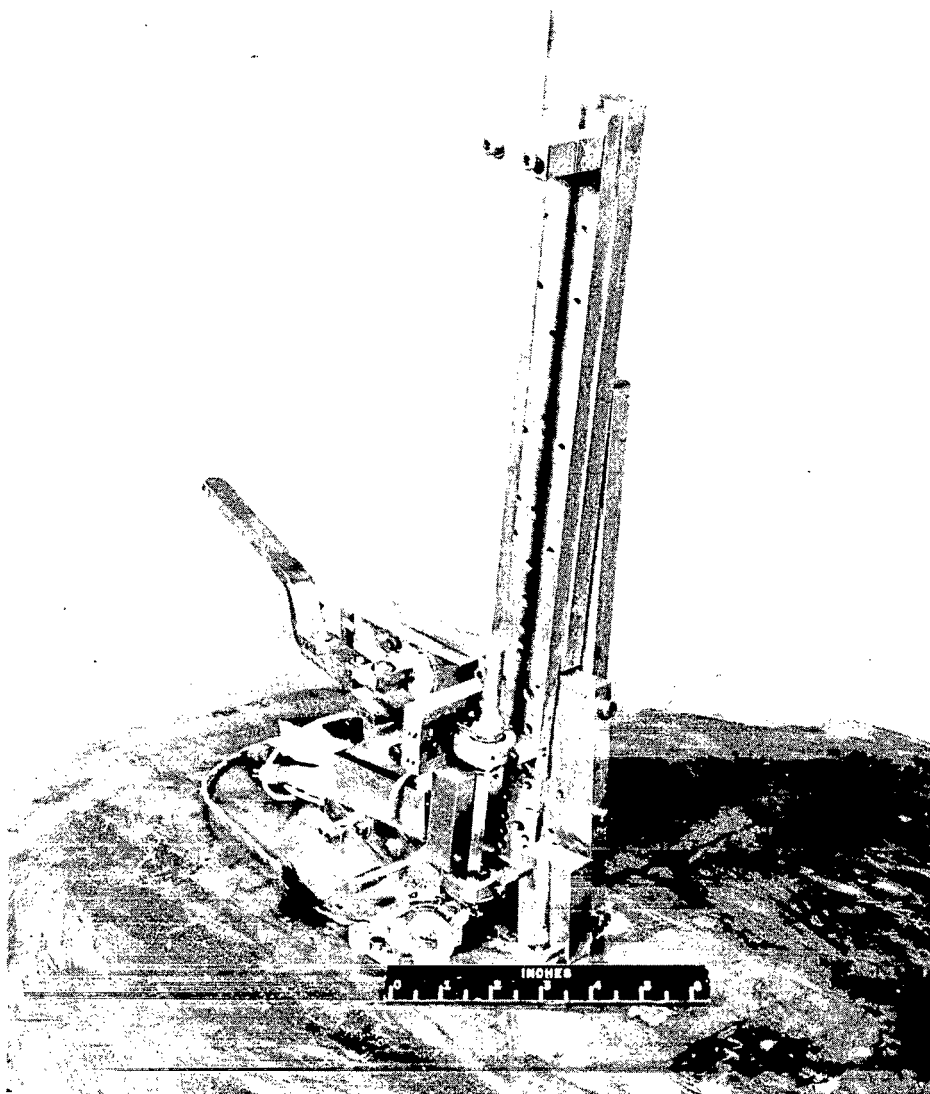
(b) Details of various control profiles tested.

Figure 2.- Concluded.



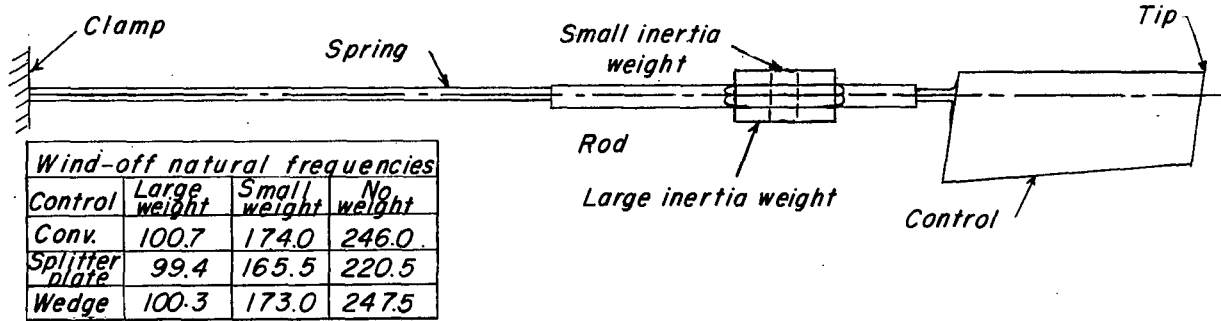
(a) General arrangement of model and reflection plate. L-86715

Figure 3.- Photographs of test installation.



(b) Rear view of reflection plate showing test components. L-96431

Figure 3.- Concluded.



Wind-off natural frequencies			
Control	Large weight	Small weight	No weight
Conv.	100.7	174.0	246.0
Splitter plate	99.4	165.5	220.5
Wedge	100.3	173.0	247.5

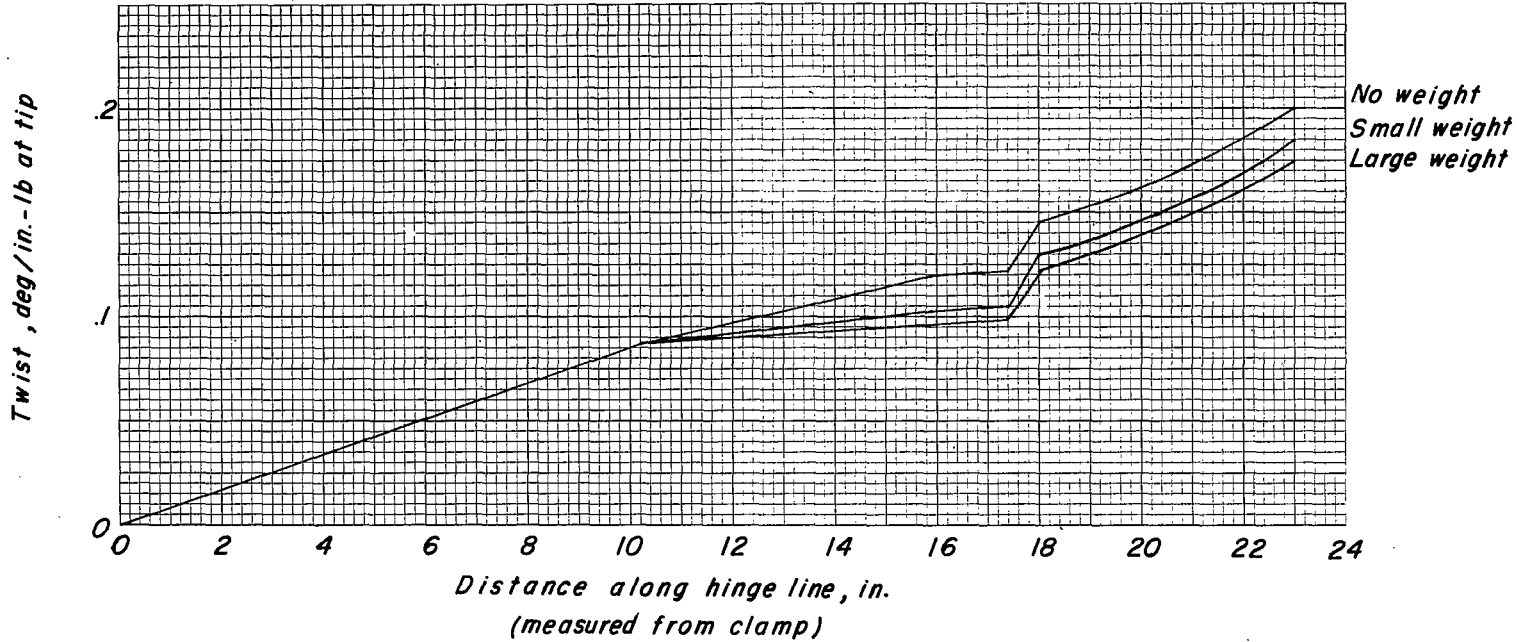


Figure 4.- Control system stiffness and frequency for various controls and inertia weights.

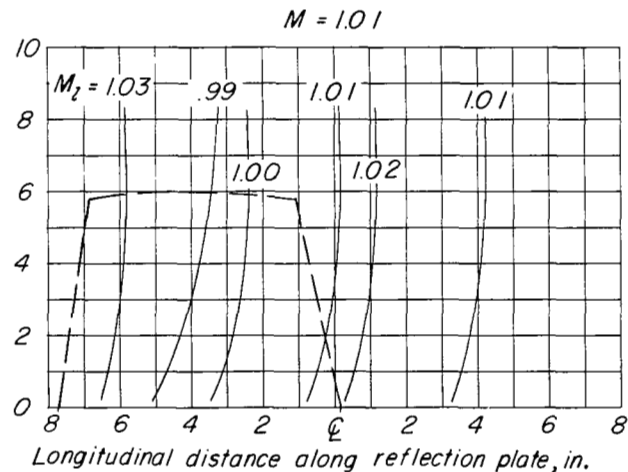
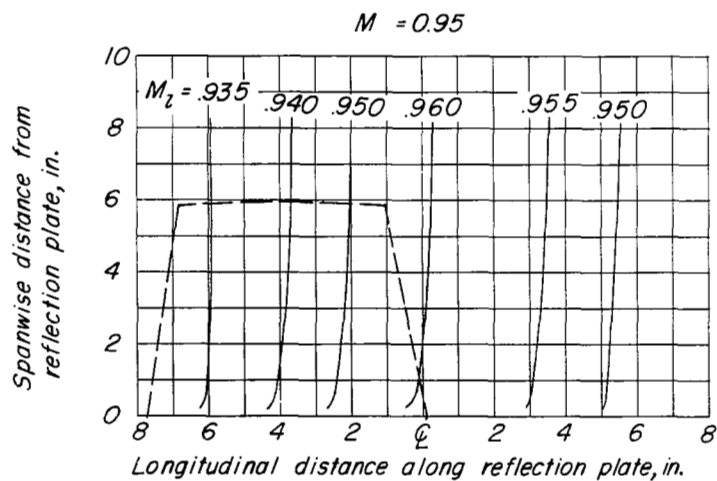
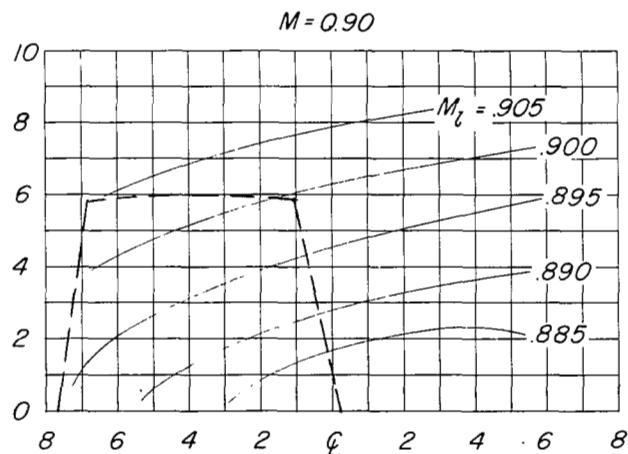
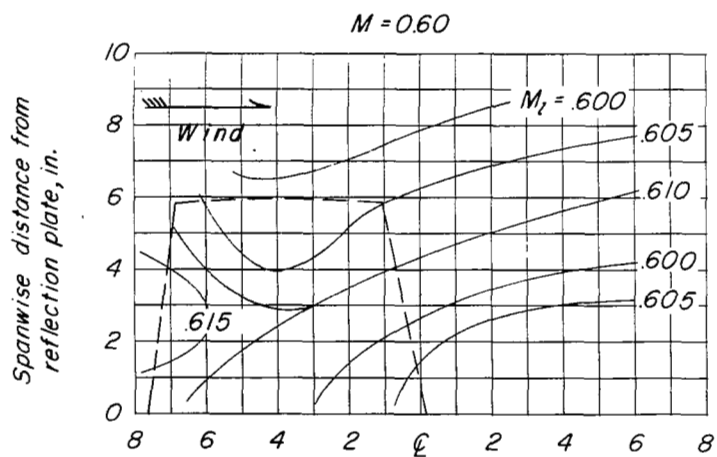


Figure 5.- Typical Mach number contours across reflection plate in vicinity of model location.

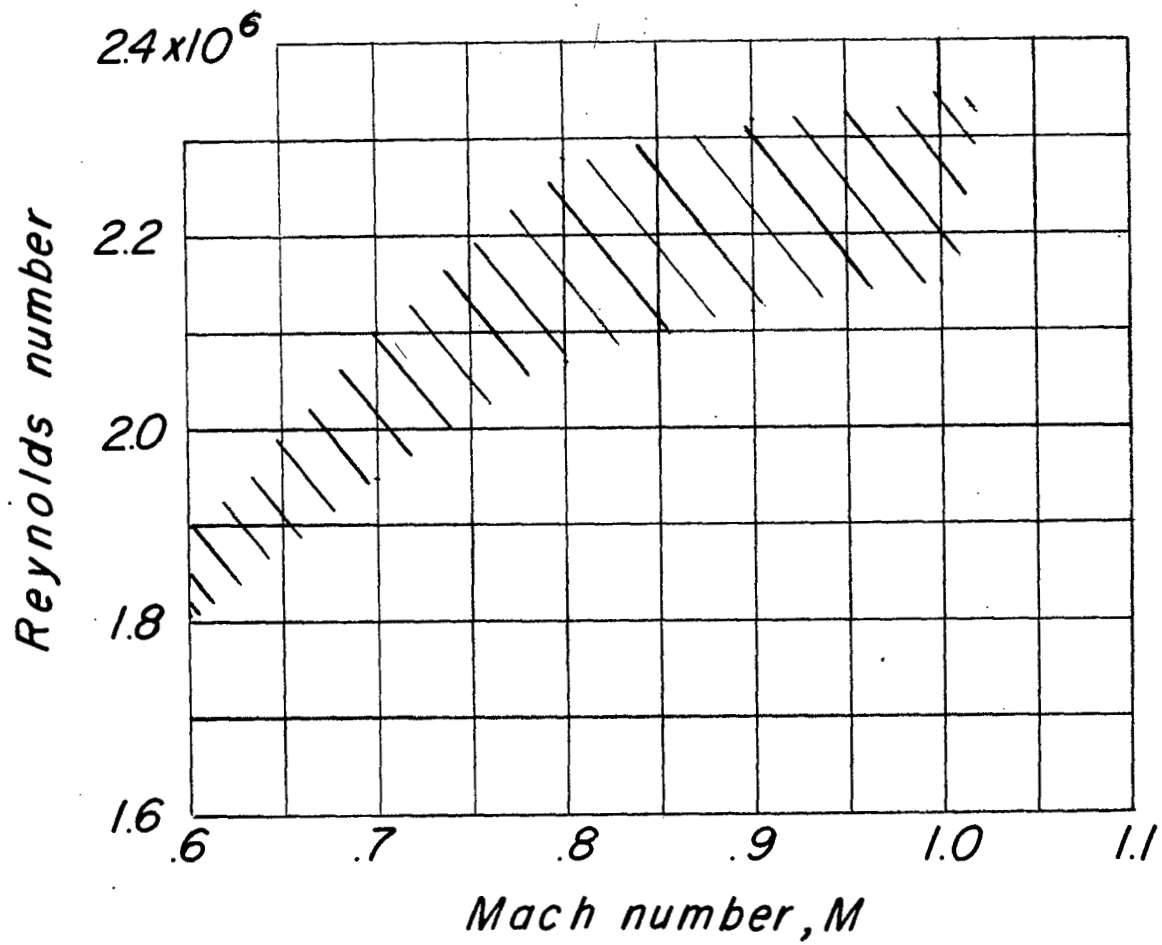
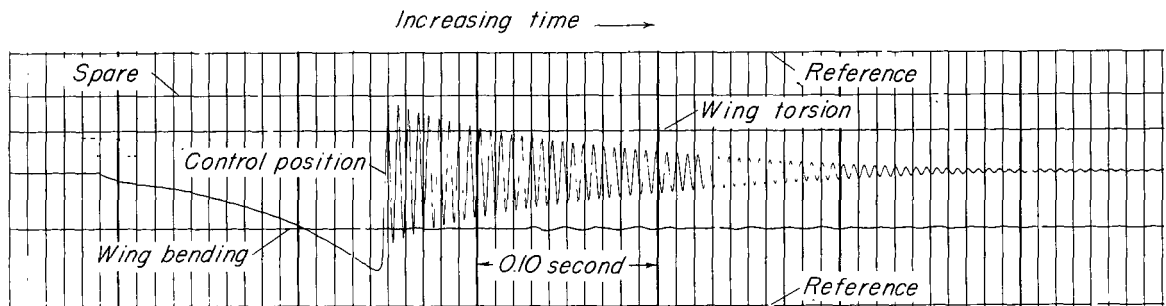
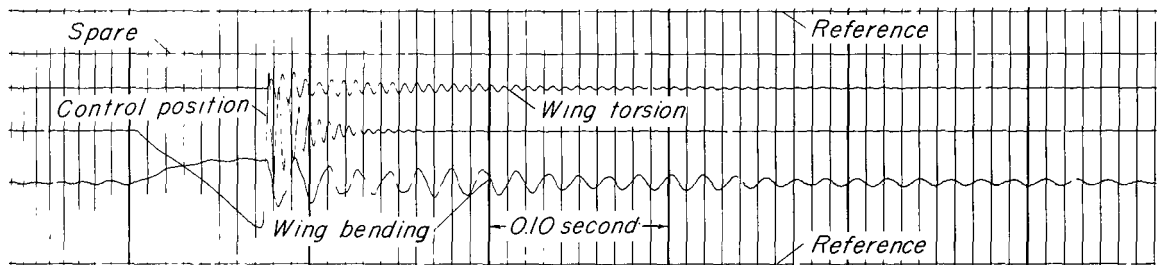


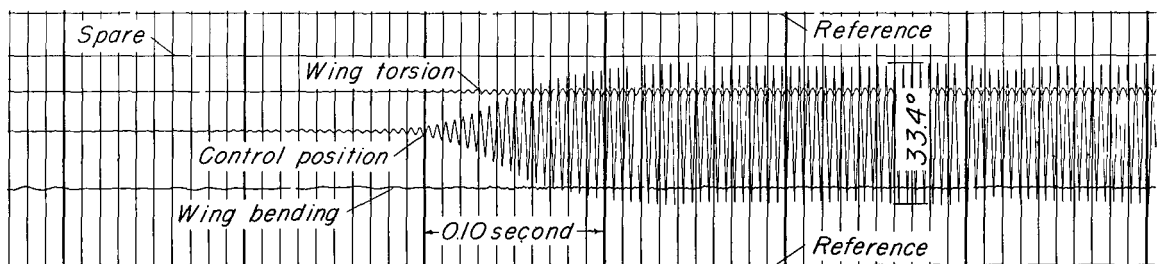
Figure 6.- Variation of Reynolds number with Mach number.



(a) Wind off, control released at $\delta \approx 10^\circ$.

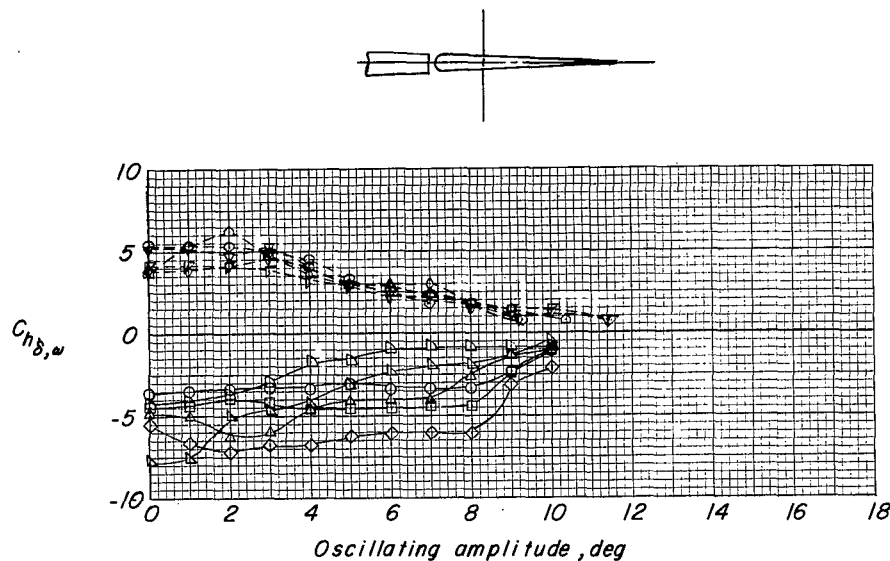


(b) $M = 0.70$, control released at $\delta \approx 10^\circ$.

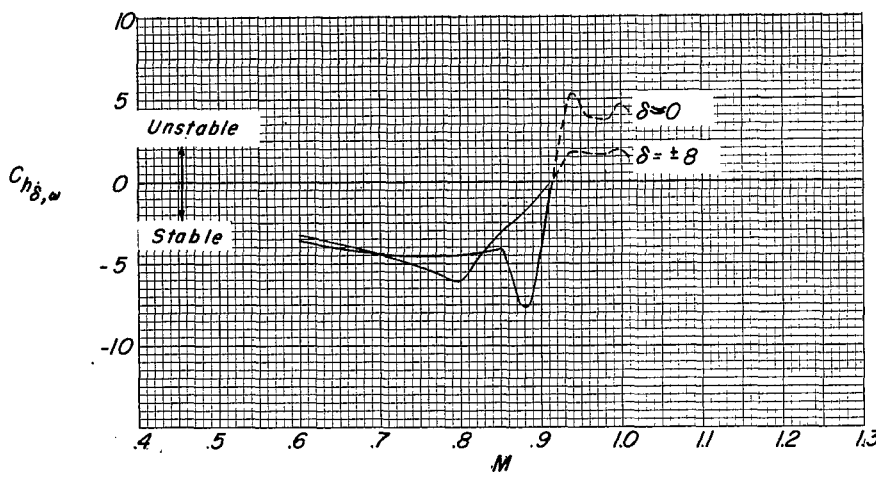


(c) $M = 1.00$, control released at $\delta \approx 0^\circ$.

Figure 7.- Typical oscillograph records. Heavy tip-store; $\alpha = 0^\circ$;
 $f_o = 174$ cps; $c_b/c_a = 0.35$.



M	k
○ 0.60	.195
□ 0.70	.171
◇ 0.80	.150
△ 0.85	.144
▽ 0.88	.144
◇ 0.90	.139
◇ 0.94	.137
◇ 0.96	.136
◇ 0.98	.134
△ 1.00	.132
▽ 1.01	.131

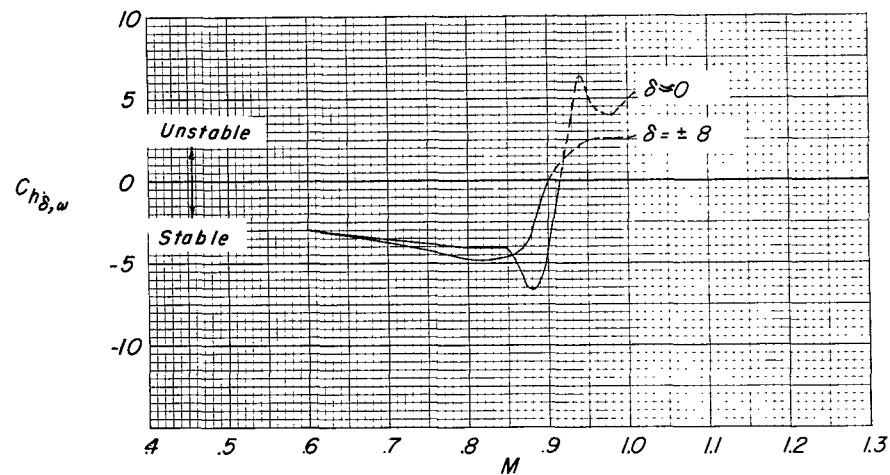
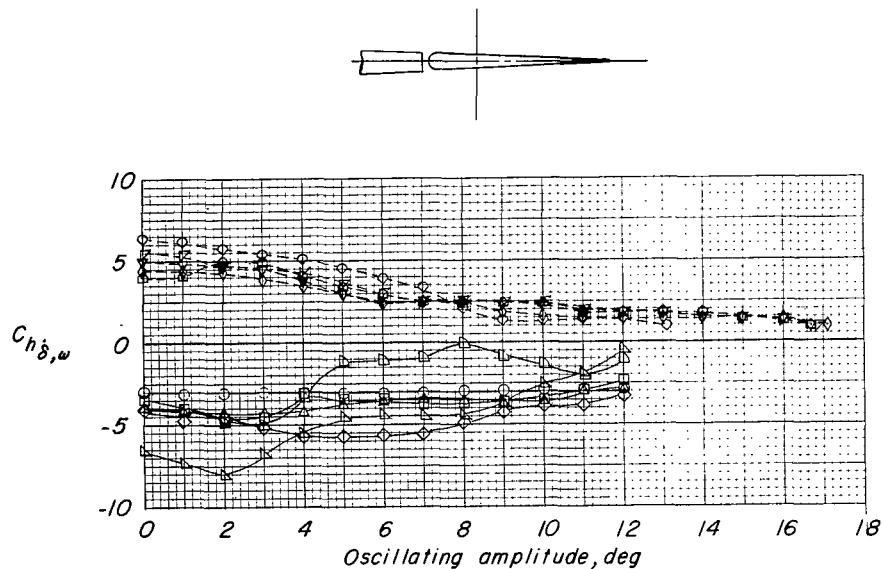


Flutter Characteristics

M	Frequency cps	Amplitude deg
0.60 to 0.90	No	flutter data
0.92	No	flutter data
0.94-S	267.0	9.30
0.96-S	270.0	9.20
0.98-S	270.0	10.35
1.00-S	271.5	11.35
1.01-S	272.5	11.50

(a) $f_0 = 246.0$.

Figure 8.- Variation of damping coefficient with oscillating amplitude and Mach number for various control frequencies. Conventional control.

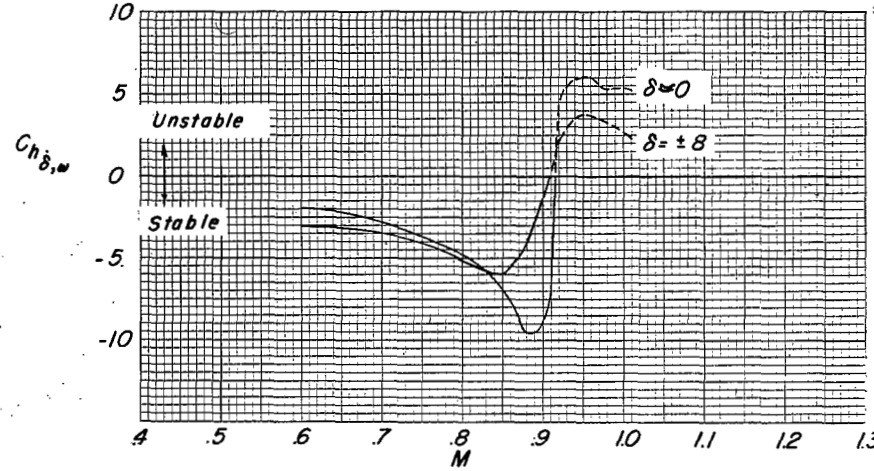
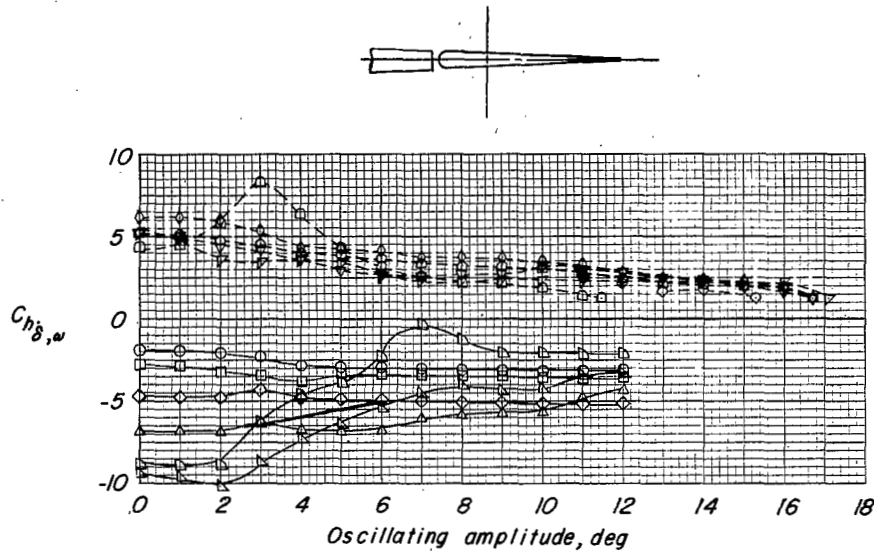


Flutter Characteristics

M	Frequency cps	Amplitude deg
0.60 to 0.90	No flutter	
0.92	No data	
0.94-S	187.2	13.10
0.96-S	189.0	17.10
0.98-S	190.2	16.70
1.00-S	191.0	16.70
1.01-S	190.7	16.90

(b) $f_0 = 174.0$.

Figure 8.- Continued.

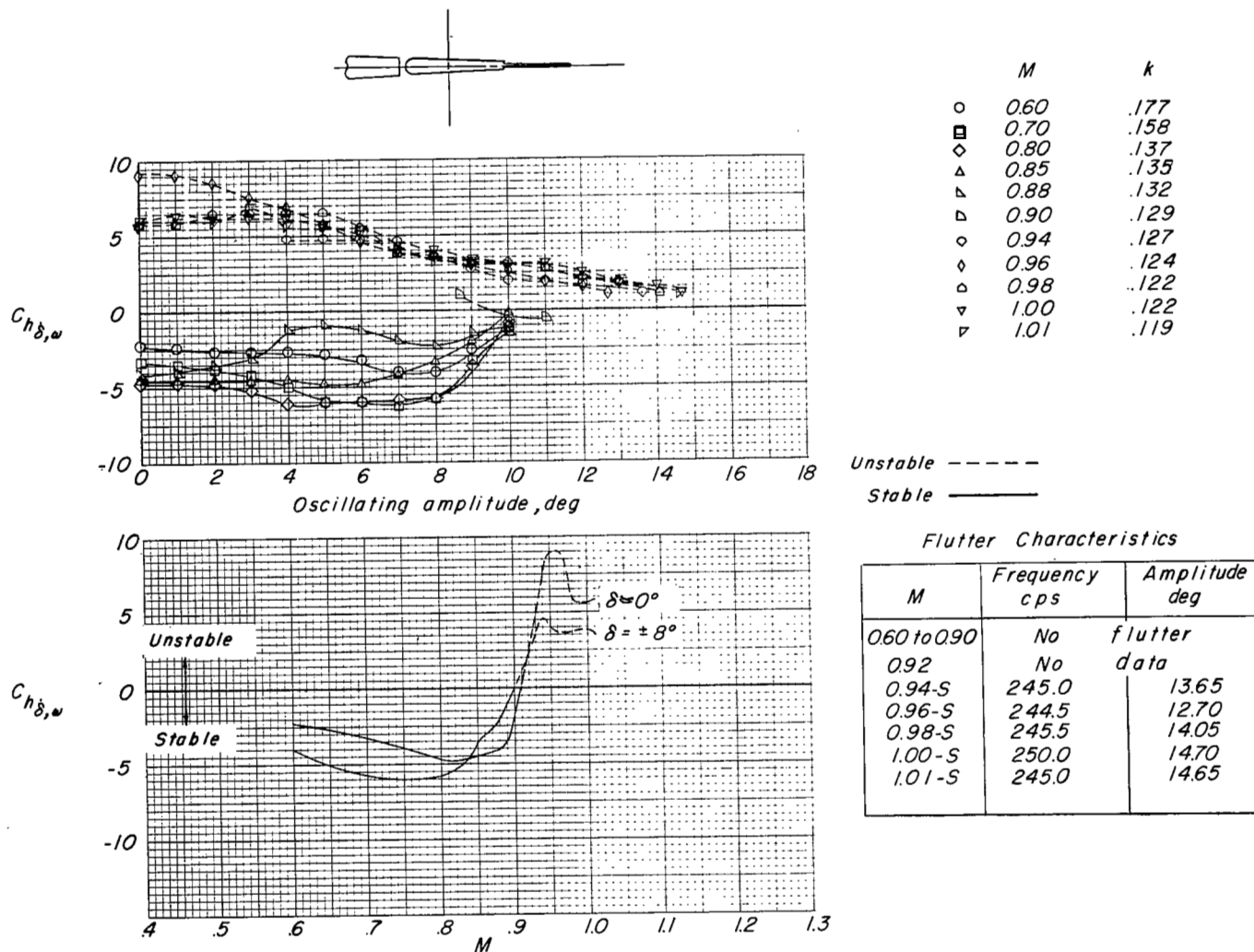


Flutter Characteristics

M	Frequency cps	Amplitude deg
0.60 to 0.90	No	flutter
0.92-S	109.5	11.45
0.94-S	108.6	15.30
0.96-S	110.3	16.70
0.98-S	109.6	16.70
1.00-S	110.3	16.70
1.01-S	110.9	17.10

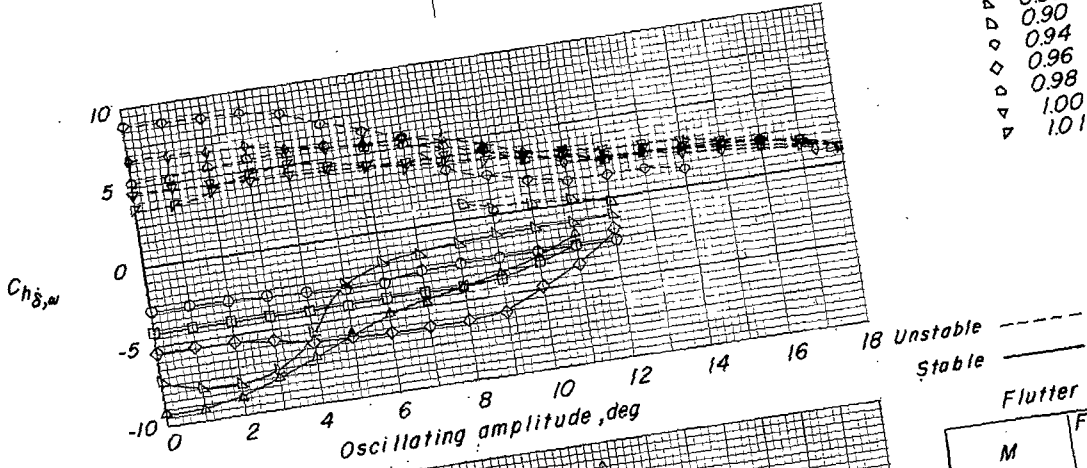
(c) $f_0 = 100.7$.

Figure 8.- Concluded.

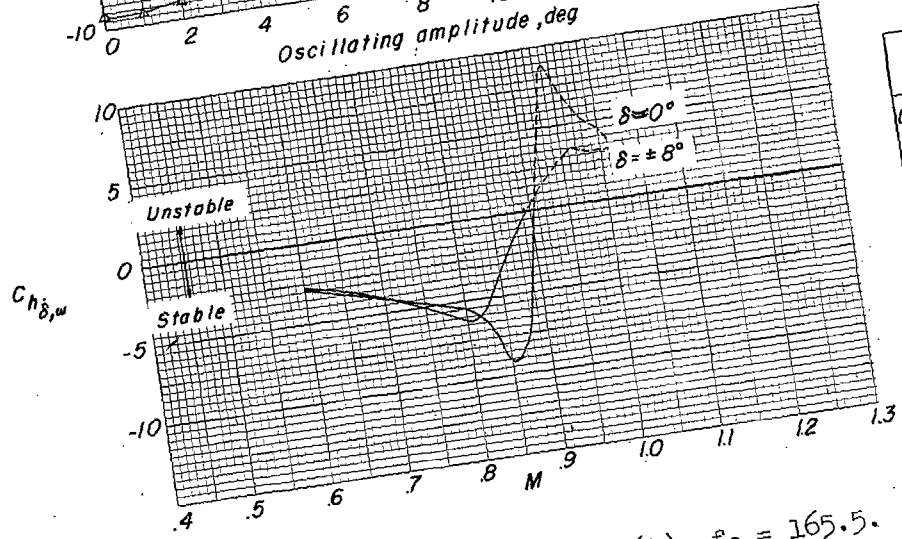


(a) $f_0 = 220.5$.

Figure 9.- Variation of damping coefficient with oscillating amplitude and Mach number for various control frequencies. Splitter-plate control.

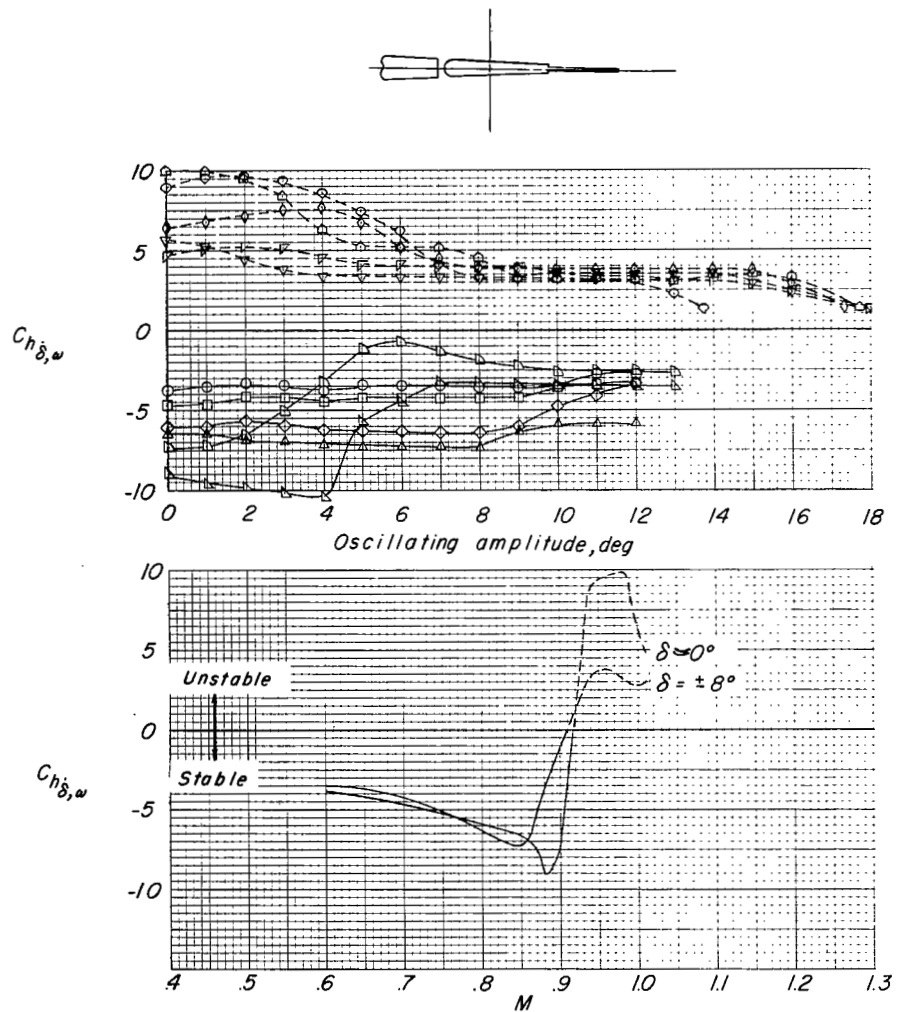


M	k
0.60	.131
0.70	.113
0.80	.101
0.85	.098
0.88	.096
0.90	.093
0.94	.093
0.96	.092
0.98	.091
1.00	.090
1.01	.089



Flutter Characteristics		
M	Frequency, cps	Amplitude, deg
0.60 to 0.90	No flutter data	14.00
0.92	181.8	17.35
0.94-S	182.4	17.75
0.96-S	182.7	18.00
0.98-S	184.5	18.15
1.00-S	185.0	

(b) $f_0 = 165.5$.
Figure 9.- Continued.



	M	k
○	0.60	.079
□	0.70	.069
◇	0.80	.060
△	0.85	.057
▽	0.88	.056
◊	0.90	.056
◇	0.94	.055
◊	0.96	.055
△	0.98	.054
▽	1.00	.053
◊	1.01	.053

Unstable - - - -
Stable - - - -

Flutter Characteristics

M	Frequency cps	Amplitude, deg
0.60 to 0.90	No flutter	
0.92	No data	
0.94-S	107.0	13.65
0.96-S	108.2	17.35
0.98-S	108.3	17.75
1.00-S	109.5	18.00
1.01-S	109.5	18.05

(c) $f_0 = 99.4$.

Figure 9.- Concluded.

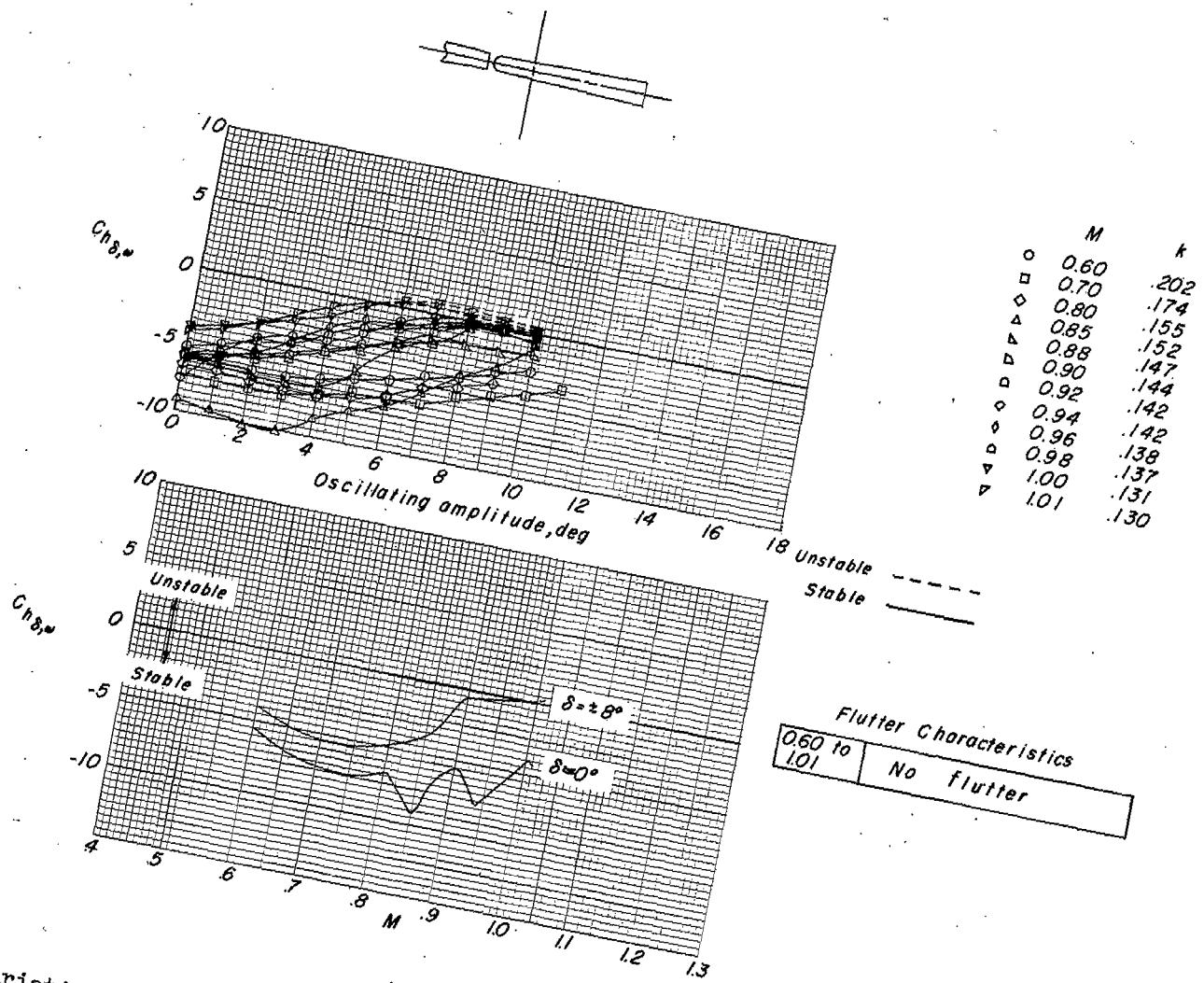
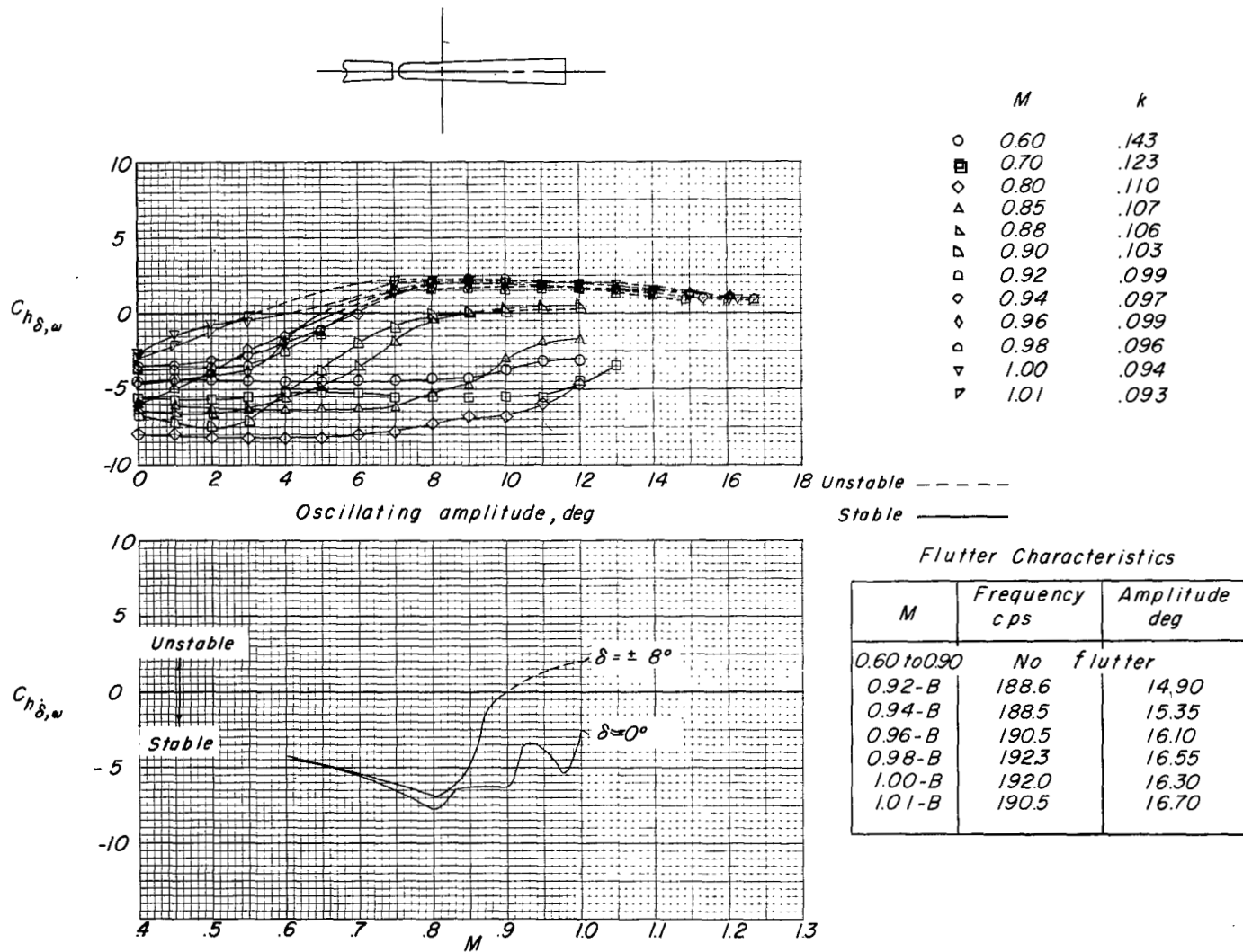


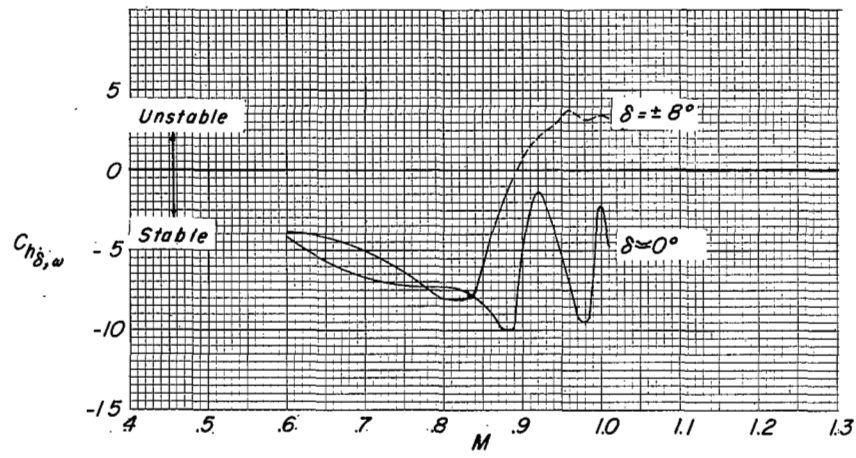
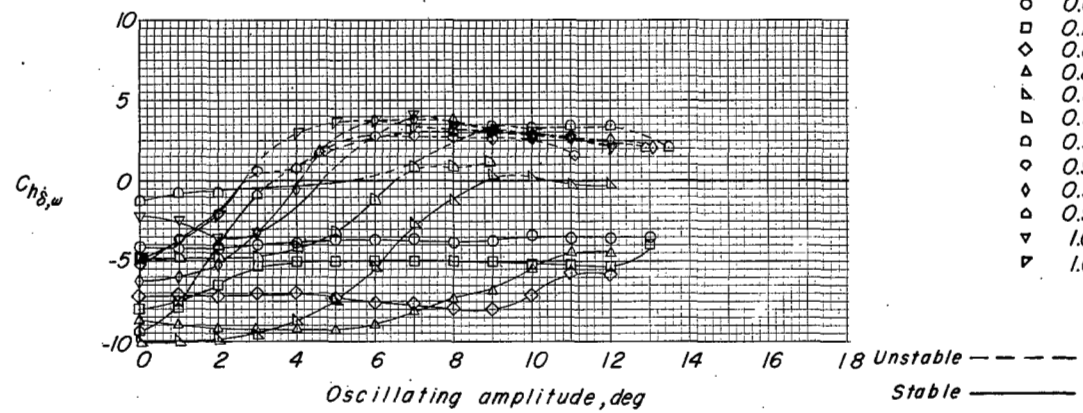
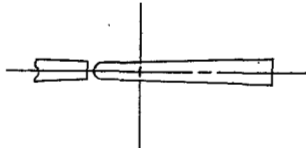
Figure 10.- Variation of damping coefficient with oscillating amplitude and Mach number for various control frequencies. Wedge control.

(a) $f_0 = 247.5$.



(b) $f_0 = 173.0$.

Figure 10.- Continued.

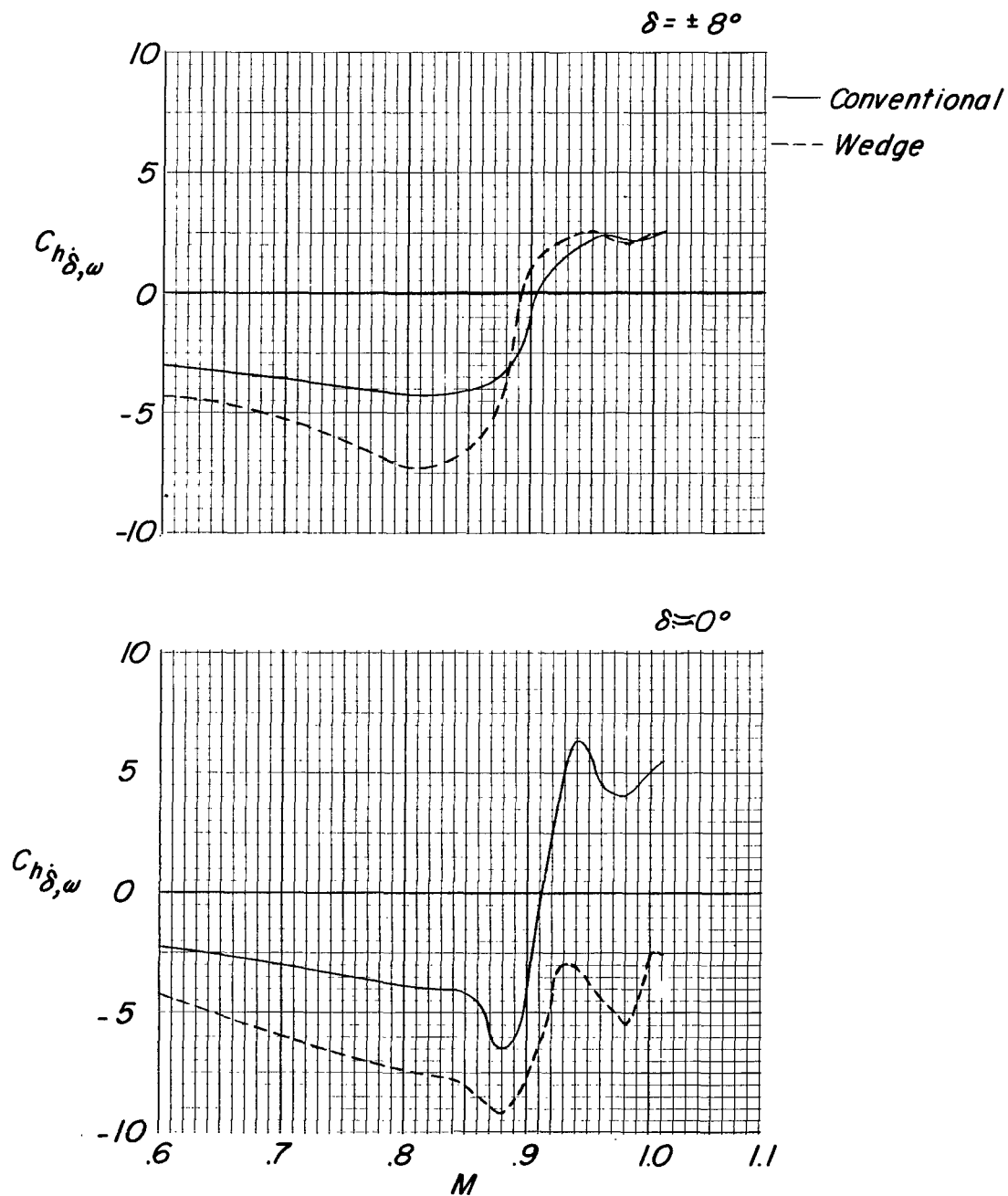


Flutter Characteristics

M	Frequency, cps	Amplitude deg
0.60 to 0.90	No flutter	
0.92-B	110.0	13.45
0.94-B	111.0	11.10
0.96-B	110.0	13.10
0.98-B	111.5	11.90
1.00-B	111.0	12.05
1.01-B	110.5	12.15

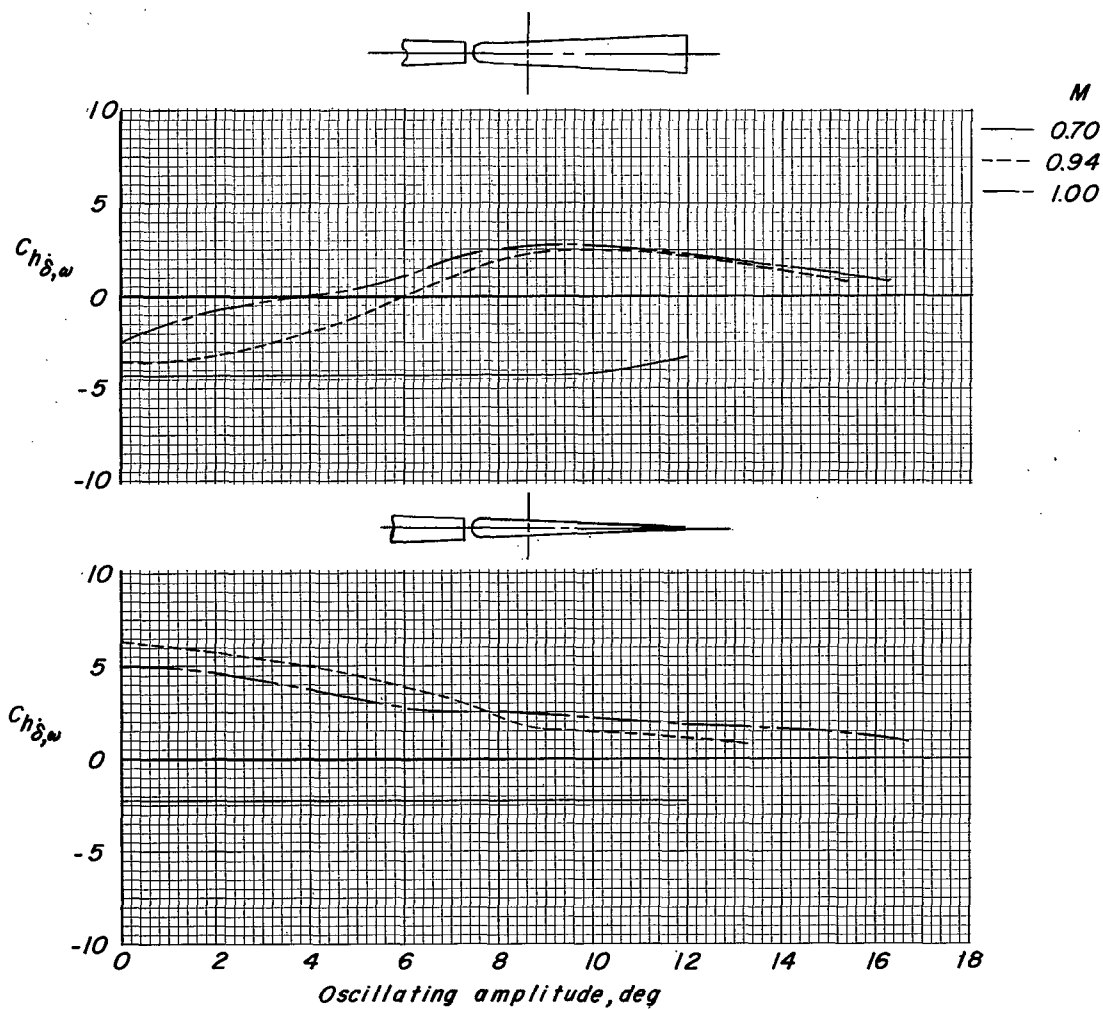
(c) $f_0 = 100.3$.

Figure 10.- Concluded.



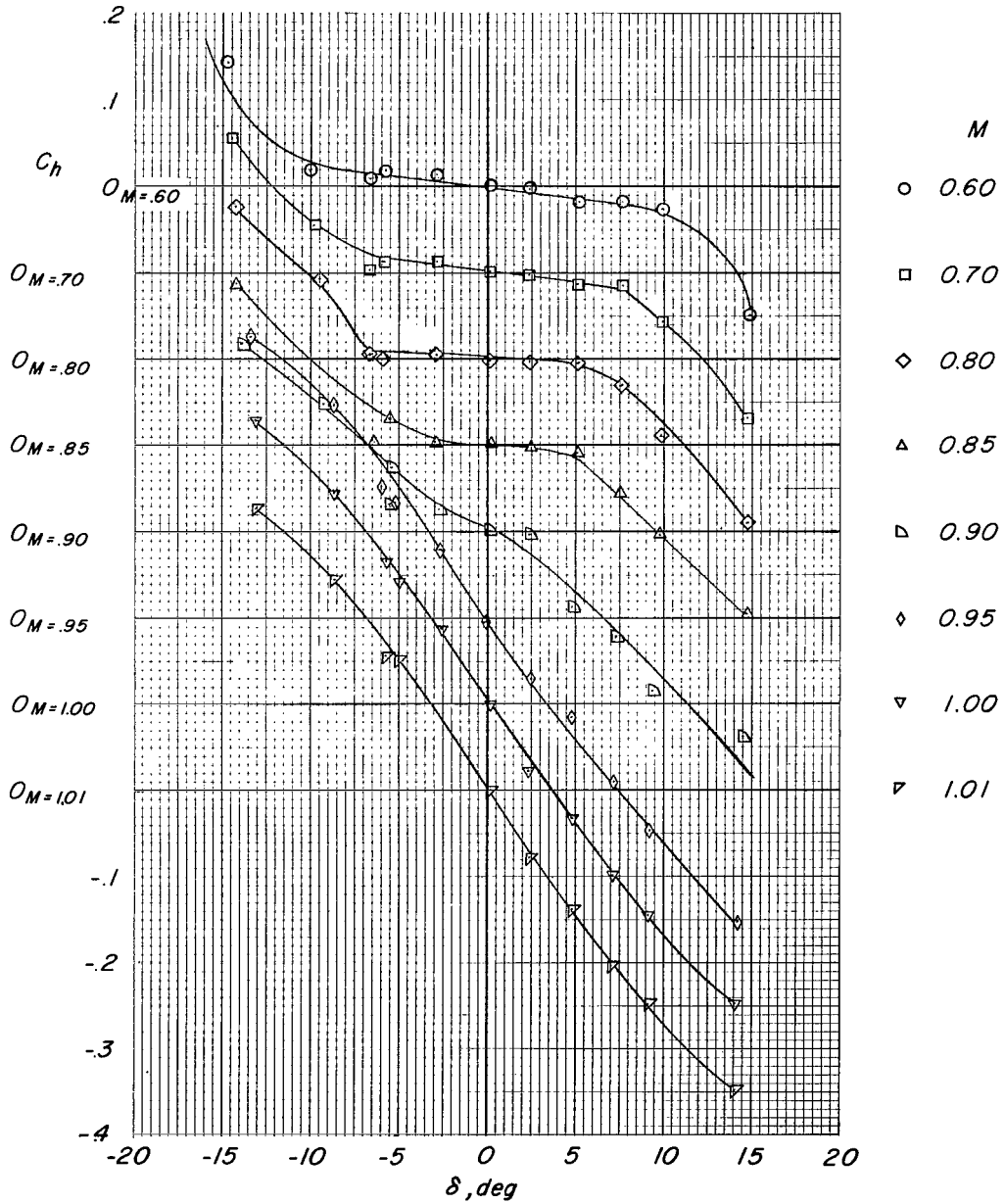
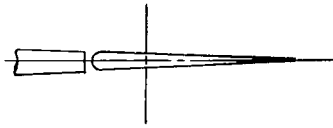
(a) Effect of Mach number.

Figure 11.- Variation of damping derivative for conventional and wedge controls. $k \approx 0.10$.



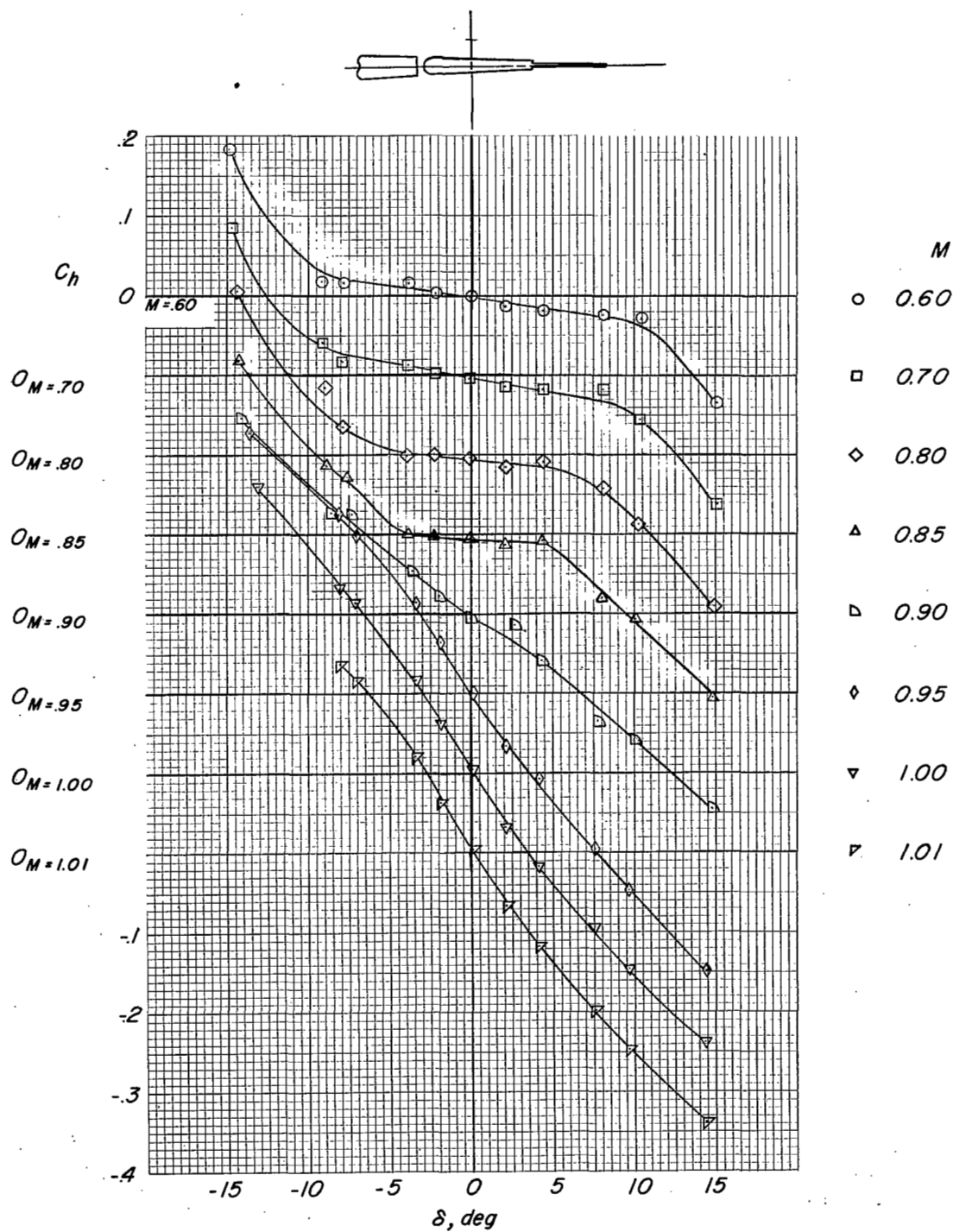
(b) Effect of oscillating amplitude.

Figure 11.- Concluded.



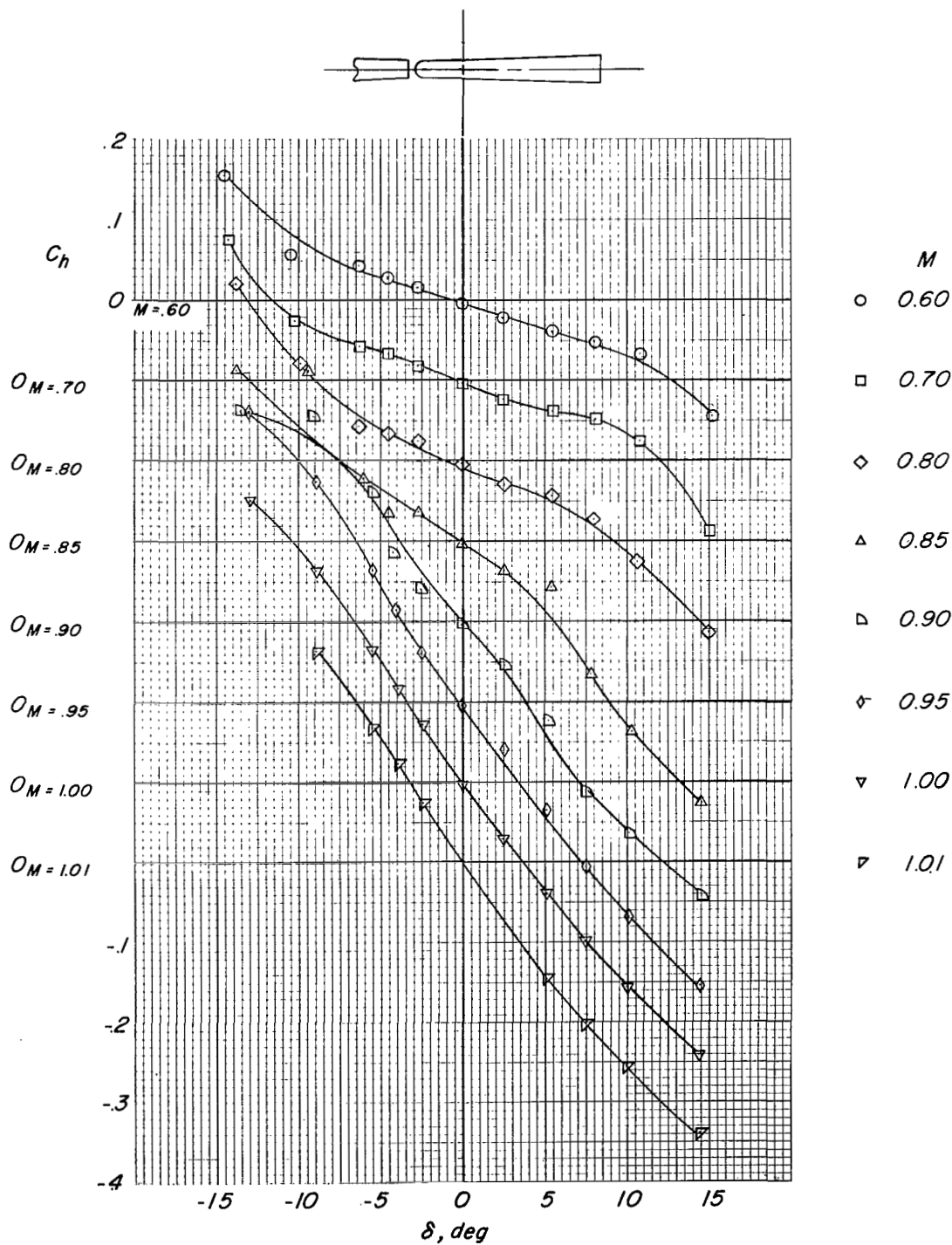
(a) Conventional control.

Figure 12.- Variation of static hinge-moment coefficient with control deflection for various Mach numbers.



(b) Splitter-plate control.

Figure 12.- Continued.



(c) Wedge control.

Figure 12.- Concluded.

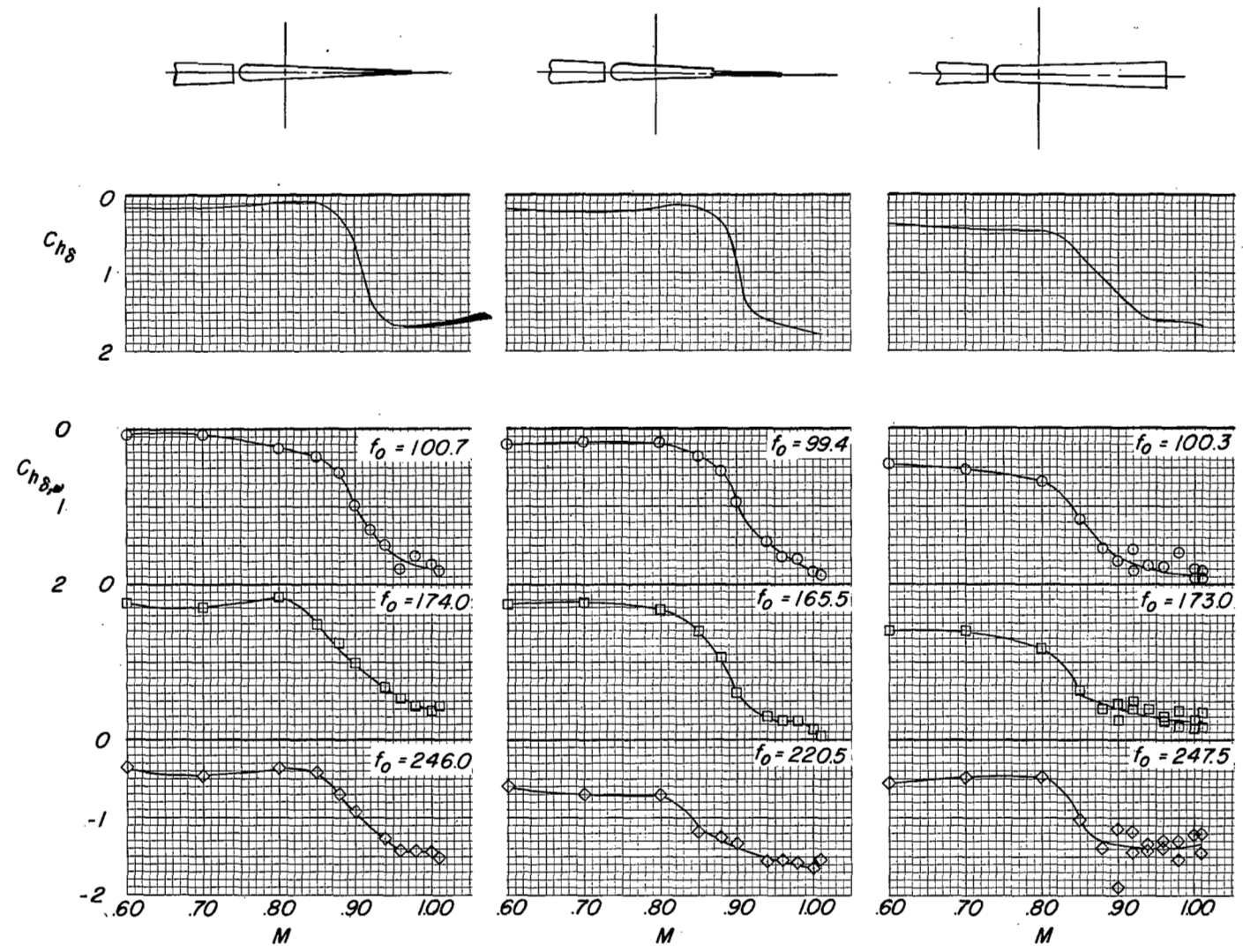


Figure 13.- Variation of $C_{h\delta}$ and $C_{h\delta,w}$ for conventional splitter-plate and wedge controls.

NASA Technical Library



3 1176 01438 1033

